Morphology and salt excretion mechanism of the salt glands in Rhodes grass (*Chloris gayana* Kunth)

A dissertation submitted in partial fulfilment
of the requirements for the degree of
Doctor of Agricultural Sciences

by

OI Takao

Laboratory of Plant Resources and Environment
Division of Bioresource Production and Agroecology
Department of Biosphere Resource Science
Graduate School of Bioagricultural Sciences
Nagoya University
Nagoya, JAPAN

March, 2014

Contents

Abbreviations

ANOVA	: analysis of variance
approx.	: approximately
BSE	: back-scattered electron
d	: day
DMSO	: dimethyl sulfoxide
DW	: dry weight
EDS	: energy dispersive X-ray spectrometry
h	: hour
LV-SEM	: scanning electron microscopy in a low-vacuum mode
min	: minute
O-D-O method	: osmium-DMSO-osmium maceration method
OsO_4	: osmium tetroxide
Pa	: Pascal
s	: second
SE	: standard error
SEM	: scanning electron microscopy
TEM	: transmission electron microscopy

General Introduction

Salt accumulation in soil is one of the most serious environmental factors limiting the growth and yield of crop plants (Hillel 2000). Salinity in the soil solution can be derived from geochemical sources, seawater intrusion into ground waters, seawater salts in wind and rain, excess application of fertilizer to farmland, and irrigation with salt-containing waters (Neumann 2011). Worldwide, more than 800 million hectares of land are estimated to be salt affected (Rengasamy 2010). It is estimated that more than 6% of the world's land and 30% of the world's irrigated areas already suffer from salinity problems (Chaves *et al*. 2009). The demand for salt-tolerant crops is increasing because of the increase of salt accumulated field.

Excess salinity induces various detrimental effects on crop production, such as growth, photosynthesis, protein synthesis, and lipid metabolism (Parida and Das 2005). To cope with excess salinity, salt-tolerant plants have acquired specific mechanisms. Among such mechanisms, 'salt glands' are known as epidermal cells or trichomes specialized for excretion of excess salts from the plant body (Waisel 1972). Salt excretion is considered to be one of the salt-tolerant mechanisms regulating ion balance in the leaf tissues (Naidoo and Naidoo 1998a).

Salt glands are reported in various plant species in at least 12 plant families (Waisel 1972) and are divided into three types on the basis of their structure: the bladder cells of the Chenopodiaceae, the multicellular glands of other dicotyledonous families, and the bicellular glands of the Poaceae (Thomson *et al*. 1988; Kobayashi 2008). The bladder cell accumulates salts in its vacuole and eventually the cell ruptures releasing the salts to the outside of the leaf surface (Esau 1977; Fahn 1988). The multicellular gland is

composed of varying number of cells, from 6 to 40 or more, and excretes salts directly through pores in the surface cuticle (Esau 1977; Thomson *et al*. 1988). The bicellular gland of the Poaceae consists of an inner basal cell and an outer cap cell (Thomson *et al*. 1988). Both the basal cell and the cap cell in the Poaceae have common features at the ultrastructural level: dense cytoplasm, abundant mitochondria, undeveloped plastids, and small vacuoles of varying size (Thomson *et al*. 1988; Kobayashi 2008). The basal cell is assumed to be the salt-collecting cell, and the cap cell is assumed to be the salt-excreting cell (Liphschitz and Waisel 1974; Kobayashi 2008). However, the pathway of solute movement in the two gland cells is not well understood.

The bicellular salt gland in the Poaceae is considered to be a 'microhair' on the basis of plant anatomy. The microhair is a bicellular trichome and found in almost all the Poaceae, except for the subfamily Pooideae (Tateoka *et al*. 1959; Clayton and Renvoize 1986). In salt tolerant plants, the bicellular hairs are termed 'microhairs' by anatomists and 'salt glands' by physiologists (Liphschitz and Waisel 1974; Amarasinghe and Watson 1988). The salt-excreting microhairs, bicellular salt glands, have been reported to be present in at least 16 genera of the Poaceae (Oross *et al*. 1985; Kobayashi 2008). Most of these genera belong to the subfamily Chloridoideae (Kobayashi 2008). Although staple crops belonging to the subfamily Oryzoideae (e.g. rice) and to the subfamily Panicoideae (e.g. maize, sorghum, and millet) also possess microhairs (Clayton and Renvoize 1986), the microhairs in these crops have little ability of salt excretion. Because the Poaceae includes many important crops and forage species, to study the details of the bicellular salt glands and to modify microhairs of salinity-sensitive crop species as salt glands would be one of the approaches to improve salt tolerance.

Rhodes grass (*Chloris gayana* Kunth), which belongs to the subfamily Chloridoideae in the Poaceae, is known to excrete salts on the leaf surfaces (Liphschitz *et al*. 1974; Kobayashi *et al*. 2007; Kobayashi and Masaoka 2008). This grass is a widespread popular fodder as pasture or hay because of its luxuriant development and environmental tolerance, and is considered particularly useful in saline areas because of its salt tolerance (Suttie 2000). Recently, physiological features of the salt excretion in Rhodes grass were studied in detail (Kobayashi *et al*. 2007; Kobayashi and Masaoka 2008). These studies indicated that the salt excretion of Rhodes grass leaves is energy-consumptive and cation-selective process. Because knowledge and information from both agricultural and biological point of views are available, Rhodes grass is expected to be appropriate for the study of bicellular salt glands in the Poaceae. However, the morphology and ultrastructure of the salt glands of Rhodes grass have not been studied in detail.

In this thesis, I investigated the morphology and ultrastructure of the salt glands on the leaves of Rhodes grass by electron-microscopy and discuss their salt-excretion mechanism (Chapter 1). To show that the bicellular glands of Rhodes grass really excrete salts as water droplets, I attempted to observe fresh leaf surfaces at the electron-microscopic level (Chapter 2). Since the result of this study suggests that the bicellular glands of Rhodes grass excrete salt-containing water without pores on the cuticle of the cap cells, I investigated the surface microstructure of the cuticle of the cap cells (Chapter 3). Based on the results, I discuss the excretion process of the salt-containing water through the cuticle of the cap cell.

Chapter 1

Morphology and ultrastructure of the salt glands on the leaf surface of Rhodes grass

The contents were published in

Oi *et al*. (2012) *International Journal of Plant Sciences* 173: 454–463.

http://www.jstor.org/stable/10.1086/665588

Introduction

The salt gland in the Poaceae is grouped in one of the trichomes. Trichomes developed outward on the surfaces of plant organs and vary in size, shape, and location among plant species (Werker 2000; Kobayashi *et al*. 2010). They play diverse roles, such as reflecting radiation, reducing leaf wetness, protecting the plant from herbivores, secreting substances, and excreting salts (Werker 2000; Kobayashi *et al*. 2010). Poaceae plants have several different types of trichomes, such as prickles, macrohairs, and microhairs (McWhorter *et al*. 1993; Kobayashi *et al*. 2010). The prickle is a structure with a protuberant base and a sharp apex. The macrohair is generally long enough to observe with the naked eye. The microhair is bicellular and found in almost all the Poaceae, except for the subfamily Pooideae (Clayton and Renvoize 1986; Amarasinghe and Watson 1988). In some salt tolerant Poaceae plants, microhairs are considered to function as salt glands.

Although the bicellular salt glands, microhairs, are distributed on leaf or stem surfaces (Kobayashi 2008), the distribution pattern and detailed location of bicellular salt glands are not well characterized in the Poaceae. In addition, cells of the salt glands are thought to be highly specialized for compartmentation, transport, and excretion of salts (Lüttge 1971), however, the salt-excretion mechanism of the bicellular glands is not well understood.

Rhodes grass belongs to the subfamily Chloridoideae in the Poaceae and is known to excrete salts on the leaf surfaces (Liphschitz *et al*. 1974; Kobayashi *et al*. 2007; Kobayashi and Masaoka 2008). Previously, ion-excretion ability of leaves of Rhodes grass has been investigated in detail (Kobayashi *et al*. 2007; Kobayashi and Masaoka

2008), whereas the morphology and ultrastructure of the salt glands of Rhodes grass has not been studied well.

In this chapter, I examined the morphology, distribution, and ultrastructure of salt glands of Rhodes grass to obtain insight into the response of the bicellular salt glands to salinity and into the salt-excretion mechanism.

Materials and Methods

Plant growth conditions and salt treatments

Caryopses of Rhodes grass (*Chloris gayana* Kunth 'Katambora') were germinated on culture soil in 300-mL plastic pots in a growth chamber. The cultivation condition was controlled at 30°C/25°C (light/dark), relative humidity of 60%, 14-h photoperiod, and light intensity of 500 μmol m^{-2} s^{-1}. Following germination, three seedlings per pot were left by thinning and were grown with tap water. After 7 d of growth, salt treatment was started by supplying NaCl solution: the concentrations were 0, 50, 100, 200, 300, and 400 mM, and each pot was supplied with 50-mL solution every day for 14 d.

Ion analysis

The sixth leaves of Rhodes grass were used for ion analysis. At the end of 7 d of NaCl treatment, when all of the sixth leaves were fully expanded, they were thoroughly washed with distilled water to remove salts and other contaminants on the surfaces. At the end of 14 d of NaCl treatment, the sixth leaf blades were excised and inserted into a test tube containing 10 mL of distilled water one by one, and were shaken for 3 min to be rinsed. The rinsing solutions were retained for excreted-ion analysis. The leaf blades

were dried at 70°C for 48 h and weighed. The dried leaf blades were powdered and extracted in 1 M HCl at room temperature for 72 h. After being filtered, the extracting solutions were retained for analysis of ion contained within the leaf blades. The concentrations of Na^+ and K^+ in rinsing and extracting solutions were analysed with an atomic absorption spectrometer (AA-6400F, Shimadzu, Kyoto, Japan).

Scanning electron microscopy (SEM) observation

Specimens for SEM were made from the tenth leaves of Rhodes grass at the end of NaCl treatment for 14 d. The leaves had not appeared at the beginning of NaCl treatment and were fully expanded at the end of treatment. Small segments (approx. 3 mm × 5 mm) were excised from the middle portion of the leaf blades and were fixed in 5% glutaraldehyde in 50 mM sodium phosphate buffer (pH 7.2). The segments were rinsed with the buffer and distilled water, dehydrated in a graded ethanol series (30, 50, 70, 90, 99, and 100%), treated with isoamyl acetate, and then dried using a critical-point dryer (HCP-2, Hitachi, Tokyo, Japan). They were coated with gold using a sputter coater (IB-3, Eiko, Tokyo, Japan) after being mounted on a stub with adhesive carbon tape. The specimens were then observed with a scanning electron microscope (S-4200K, Hitachi) at an accelerating voltage of 15 kV.

The number of salt glands was counted on scanning electron micrographs at 100-fold magnification (an area of 1.05 mm^2). The micrographs were taken from leaf surfaces except the midrib and blade margins. The density (number per mm^2) of salt glands was estimated from the number counted in a micrograph. Total number of salt glands per leaf was calculated as the product of the density and the total leaf area. Stomata were also counted in the same way.

SEM observation with freeze cracking (O-D-O method)

To observe the intracellular structures of salt gland cells three-dimensionally, freeze cracked leaves were observed by SEM based on the osmium-DMSO-osmium maceration method (O-D-O method) (Tanaka and Naguro 1981).

Specimens were prepared from the sixth leaves of Rhodes grass grown for 21 d without NaCl treatment. Small segments (approx. 3 mm × 5 mm) were excised from the middle portion of the leaf blades, fixed in 2% paraformaldehyde + 2% glutaraldehyde in 50 mM sodium phosphate buffer (pH 7.2) at 4°C overnight, and postfixed in 1% osmium tetroxide (OsO_4) in the same buffer at 4°C for 2 h. After being rinsed with the buffer, the segments were immersed in a series of dimethyl sulfoxide (DMSO) in the buffer (15, 25, and 50%, two times for 20 min each). They were then frozen on a metal plate chilled with liquid nitrogen and were cracked into two halves with a blade and a hammer, using a freeze-cracking apparatus (TF-1, Eiko). The cracked pieces were immediately placed in 50% DMSO at room temperature. After thawing, the pieces were rinsed in the buffer until DMSO had been removed. They were then transferred in 0.1% OsO_4 in the same buffer and were left standing at 20°C for 48–72 h to remove the cytoplasmic matrix. The pieces were fixed again in 1% OsO_4 in the buffer at 4°C for 1 h. After being rinsed with the buffer and distilled water, they were dehydrated, critical-point dried, coated with gold, and then observed with a scanning electron microscope (S-4200K, Hitachi), as described above (*see SEM observation*).

Transmission electron microscopy (TEM) observation

Specimens for TEM were made from the sixth leaves of Rhodes grass at the end of NaCl treatment for 14 d. Small segments (approx. 1 mm × 2 mm) excised from the

middle portion of leaf blades were fixed in 5% glutaraldehyde in 50 mM sodium phosphate buffer (pH 7.2) and postfixed in 2% OsO_4 in the same buffer. The segments were rinsed with the buffer and distilled water, dehydrated in a graded acetone series (30, 50, 70, 90, 99, and 100%), treated with propylene oxide, and then embedded in Spurr's resin (Spurr 1969). Ultrathin sections (80–90 nm) were cut with a diamond knife and placed on 200-mesh copper grids. The grids were double stained with 2% uranyl acetate for 20 min followed by lead citrate for 5 min. The specimens were then observed with a transmission electron microscope (H-7500, Hitachi) at an accelerating voltage of 15 kV.

Other microscopy

Intact leaf surfaces were observed, and video images were obtained with a digital stereoscopic microscope (KH-7700, Hirox, Tokyo, Japan).

Specimens for light microscopy were made from embedded materials for TEM. Semithin sections (1 μm) cut with a glass knife were stained with mixed solution of 0.5% (w/v) toluidine blue and 1.5% (w/v) sodium carbonate (1:1) for 3 min. After being rinsed with distilled water and dried, the sections were observed with a light microscope (BX51, Olympus, Tokyo, Japan).

Statistical analysis

Data obtained from the experiments were statistically analysed by one-way ANOVA and Tukey's honestly significant difference test using SPSS 14.0 for Windows.

Results

Salt excretion

Droplets and crystals were observed on the leaf surfaces of Rhodes grass treated with 400 mM NaCl for 7 d (Fig. 1-1). Leaf surfaces became wetter with excreted droplets within 3 d after the beginning of NaCl treatment. Water droplets on the leaf surfaces changed into salt crystals by evaporation of water. The size of crystals increased day after day. In Rhodes grass without NaCl treatment, droplets also appeared on the leaf surfaces, but crystals did not. NaCl treatments increased Na^+ excretion and decreased K^+ excretion (Fig. 1-2a) with a concomitant increase of Na^+ content and decrease of K^+ content in the leaves (Fig. 1-2b). The tendency was more prominent in the excretion than in the content.

Leaf surface morphology and salt gland distribution

Three types of trichomes existed on the leaf surface of Rhodes grass: salt glands, macrohairs, and prickles (Fig. 1-3). Salt glands were globular in shape, shorter than other trichomes and consisted of two cells (*see below*). Macrohairs were long enough to observe with the naked eye. Prickles showed a spine shape with a protuberant base and a sharp apex.

Inclined angle viewing of leaf surfaces with cross sections showed the relation between salt gland distribution and vein location (Fig. 1-4a, b). Although the salt glands seemed to be distributed randomly because of their varied individual distance, they were distributed parallel with veins. The salt glands on the adaxial surface existed on the lines just above the small veins (Fig. 4a, c). In contrast, the salt glands on the abaxial surface existed on the lines between veins (Fig. 1-4b, d). Macrohairs were distributed on the

same lines as salt glands. Prickles on both surfaces distributed on the lines just above the veins.

Salt gland density and total number per leaf

Salt gland density increased significantly with NaCl treatment (Fig. 1-5a). When treated with 300 mM, the salt gland density on the adaxial surface was 168% of control, and the density on the abaxial surface was 152%. Although stomatal density also increased on both surfaces under treatment with 100 mM NaCl, the densities did not change between 100 and 300 mM NaCl treatment (Fig. 1-5b). Leaf area tended to be reduced with NaCl treatment. To avoid the effect of reduction in leaf area, the total number per leaf of salt glands and stomata was calculated as the product of the density and the leaf area (Fig. 1-5c). The total number of salt glands treated with 300 mM NaCl increased significantly on the adaxial surface and tended to increase on the abaxial surface. In contrast to salt glands, the total number of stomata on both surfaces did not change with the NaCl treatment.

Salt gland morphology

In the external observation of salt glands on the leaf surfaces, the head of a salt gland, the cap cell, was smooth and globular in shape and was exserted from epidermis (Fig. 1-6 *CC*). The diameter of the cap cell was approximately 15 μm. The basal cell under the cap cell was partly observed by inclined angle viewing (Fig. 1-6b *BC*). Each salt gland was surrounded by four epidermal cells (Figs. 1-3, 1-6, and 1-7). The shape and size of salt glands were not much different between the adaxial and abaxial surfaces of leaves or between control and NaCl-treated plants (*data not shown*).

The ultrastructure of the salt gland of Rhodes grass was observed by TEM (Figs. 1-7, 1-8, 1-9, and 1-10). In longitudinal sections of the salt glands, the base region of the basal cell was embedded in epidermis and had contact with epidermal and mesophyll cells (Figs. 1-8 and 1-9a). The neck region of the basal cell exserted from the base region, and the apical region was in contact with the cap cell (Figs. 1-8 and 1-9a, b). Vallecula was formed between the neck region of the basal cell and epidermal cells (Figs. 1-6b and 1-9a *Va*).

The basal cell and the cap cell of salt glands contained dense cytoplasm and were distinct from adjacent cells (Figs. 1-7, 1-8, and 1-9a). Both the basal cell and the cap cell did not have the central vacuole and chloroplasts (Figs. 1-8 and 1-9), whereas they had small vacuoles, undeveloped plastids, and abundant mitochondria (Fig. 1-9). In the basal cell, distinctive double membranes, the partitioning membranes, were observed. The partitioning membranes extended throughout the cytosol in the basal cell and linked with the plasma membrane at the common cell wall between the basal and cap cells (Fig. 1-9a, b). The cap cell did not have such double membranes (Fig. 1-9c). The cytoplasm of the basal cell was connected with adjacent cells via plasmodesmata (Fig. 1-9a, b). Plasmodesmata were observed more frequently on the common cell wall between the basal and cap cells, than on other cell walls. The external cell wall of the salt gland and epidermis were covered by a continuous cuticle (Fig. 1-9a *Cu*). The cuticle was separated from the cell wall at the top of the cap cell, and a cavity was formed (Fig. 1-9a, c *Ca*).

Paradermal sections show parts of the salt glands (Fig. 1-10). The cap cell appeared circular and had no partitioning membranes (Fig. 1-10a). The neck region of the basal cell was also circular in shape and had layered arcuate partitioning membranes

(Fig. 1-10b *arrowheads*). In the base region, the basal cell appeared oblong, and the inner space of the partitioning membranes tended to be swollen more than that in the neck region (Fig. 1-10c *arrowheads*). There was no link between the partitioning membranes and the plasma membrane in the neck and base regions. The base region of basal cell was connected with adjacent cells via plasmodesmata (Fig. 1-10c *arrows*).

There was no clear difference in the ultrastructure of salt glands between the adaxial and abaxial surfaces of leaves or between control and NaCl-treated plants (*data not shown*).

Three-dimensional ultrastructure of salt glands

In the specimens prepared by the freeze cracking method (O-D-O method), the three-dimensional ultrastructure of the basal cell of the salt glands was clearly observed by SEM (Fig. 1-11). The basal cell that was cracked partly showed the intracellular structures, such as numerous mitochondria and intricate partitioning membranes (Fig. 1-11b). The partitioning membranes extended from the upside to the underside in the basal cell, and the membranes were seen as bended sheets (Fig. 1-11 *arrowheads*). The numerous mitochondria existed between the partitioning membranes (Fig. 1-11 *asterisks*).

Discussion

Rhodes grass is known to be a salt-tolerant plant (Suttie 2000) and to excrete salts on the leaf surfaces (Liphschitz *et al*. 1974; Kobayashi *et al*. 2007; Kobayashi and Masaoka 2008). Stereoscopic microscopy showed that leaf surfaces of Rhodes grass

excreted salts in solution (Fig. 1-1). The amount of Na^+ excreted in one week (Fig. 1-2a) was nearly twice the amount of Na^+ contained in the leaf (Fig. 1-2b). Thus, Rhodes grass has the ability to efficiently excrete Na^+ from the leaf. Excretion of Na^+ increased with the increase of treated NaCl concentration, whereas excretion of K^+ decreased. Rhodes grass is considered to preferentially excrete Na^+ compared with K^+ under condition of excess Na^+. Selective excretion of Na^+ from the salt glands of Rhodes grass has been reported (Kobayashi *et al*. 2007).

Morphology and distribution of salt glands

SEM observation revealed the characteristic globular shape of salt glands (Fig. 1-6), which helps distinguish the salt glands from other surface structures and analyse their distribution on the leaf surface. Because the salt glands on the adaxial surface are located above the veins (Fig. 1-4a, c), they might adapt to excrete salts that are transported via the vessels from the root. On the other hand, the salt glands on the abaxial surface are located between the veins (Fig. 1-4b, d). The physiological significance of this distribution pattern is not known at present. The difference of the gland distribution between the surfaces may relate to the fact that the vessels are located on the adaxial side of the vein. According to Semenova *et al*. (2010), salt glands of *Distichlis spicata* (Poaceae) directly contact water-storing parenchyma cells, which accumulate salts in their vacuoles. In Rhodes grass leaves, however, such cells do not exist, and salt glands on both surfaces directly contact mesophyll cells (Figs. 1-4c, d, 1-8, and 1-9a). Interspecific difference of the salt gland distribution seems to reflect the difference in the salt-excretion pathway from the vessel to the salt gland.

Salt gland density increased with NaCl treatment (Fig. 1-5a). The number of salt glands per leaf also increased significantly on the adaxial surface (Fig. 1-5c), even though the leaf area decreased with NaCl treatment. In contrast, stomatal density increased with NaCl treatment (Fig. 1-5b); however, the number of stomata per leaf did not change (Fig. 1-5c). An increase in salt glands may be an acclimation to salinity stress, to promote salt excretion. Liphschitz *et al*. (1974) indicated that the salt gland density (per unit of leaf area) of Rhodes grass scarcely increased with 200 mM NaCl in hydroponic solution. In my preliminary experiments, NaCl treatment did not change the salt gland density on leaves that were already the fully developed uppermost leaves at the beginning of treatment (*data not shown*). In the present study, NaCl treatment did increase the salt gland density (Fig. 1-5a) on the examined leaves that had not appeared at the start of the treatment and were fully developed at the end of 14 d of treatment. These facts suggest that salinity promotes differentiation of salt glands in immature leaves.

Exogenous jasmonic acid decreases the number of salt glands and increases that of macrohairs in Rhodes grass (Kobayashi *et al*. 2010). Kobayashi *et al*. (2010) suggested that this response may be a trade-off between salt glands and macrohairs. They also suggested that macrohairs contribute to herbivore resistance and that salt glands contribute to salinity tolerance. My study showed that macrohairs exist on the same lines as salt glands (Fig. 1-4). In addition, both salt glands and macrohairs are surrounded by four epidermal cells (Figs. 1-3, 1-6, and 1-7). These facts may suggest that salt glands and macrohairs are differentiated from the same origin and support the trade-off hypothesis of Kobayashi *et al*. (2010). Differentiation of salt glands and macrohairs may be differently influenced by biotic and abiotic stresses. Further studies

on the differentiation of salt glands and macrohairs under salt stress are required to understand the adaptation of Rhodes grass to salinity stress.

Salt glands are surrounded by papillae and prickles in *Aeluropus littoralis* (Poaceae) (Barhoumi *et al*. 2008). These structures are considered to provide protection of the salt glands. Barhoumi *et al*. (2008) suggested that the salt glands are protected because they are important epidermal structures. On the other hand, the salt glands of Rhodes grass are not surrounded by papillae or prickles (Figs. 1-3 and 1-4). In addition, leaf surfaces of Rhodes grass do not have deep grooves or ridges that are observed in several Poaceae plants having salt glands, such as *Sporobolus virginicus* (Naidoo and Naidoo 1998b), *Odyssea paucinervi*s (Somaru *et al*. 2002), and *A. littoralis* (Barhoumi *et al*. 2008). Somaru *et al*. (2002) indicated that the salt glands of *O. paucinervi*s exist within the grooves and suggested that such location protects the salt glands. Protection of salt glands may not be necessary in Rhodes grass. The location and surroundings of salt glands may relate to the environment in which the plants evolved.

Ultrastructure of salt glands and the mechanism of salt excretion

The salt gland of Rhodes grass is bicellular (Fig. 1-9a), like that of other Poaceae plants, and is not tricellular as previously reported (Waisel 1972; Barhoumi *et al*. 2008). The ultrastructure of salt glands has been reported for several Poaceae species, such as *Spartina foliosa* (Levering and Thomson 1971), *Cynodon dactylon* (Oross and Thomson 1982a, 1982b), *D. spicata* (Oross and Thomson 1982b; Semenova *et al*. 2010), *S. virginicus* (Naidoo and Naidoo 1998b), *O. paucinervis* (Somaru *et al*. 2002), and *A. littoralis* (Barhoumi *et al*. 2008). These studies show that the ultrastructure of the cells constituting the salt gland has common features: high cytoplasmic density, undeveloped

plastids, abundant mitochondria, and the lack of central vacuole in both the basal and cap cells, and the existence of the partitioning membranes in the basal cell.

Membranous structures such as the partitioning membranes were not found in other parts of the plant. Therefore, the partitioning membranes are believed to have specific roles for salt transport. The inside space of the partitioning membranes are considered to be continuous with the apoplast between the cap and basal cells, thus forming the extracellular channel (Figs. 1-9b and 1-12; Levering and Thomson 1971; Oross and Thomson 1982b). In previous studies, the ultrastructure of the partitioning membranes has been shown in ultrathin longitudinal sections by TEM. In this study, I also observed paradermal sections of the salt glands (Fig. 1-10). The combination of the longitudinal and paradermal sections helps understand the three-dimensional ultrastructure of the salt gland. The partitioning membranes in the neck region of basal cell are tubules in longitudinal sections (Fig. 1-9), whereas they appear as layered arcs in paradermal sections (Fig. 1-10b). These sections suggest that the partitioning membranes exist as bended sheets in the basal cell. The layered sheet-like structures of partitioning membranes also demonstrated by SEM of the freeze cracked basal cell (Fig. 1-11). The sheets of the partitioning membranes swell in the bottom region of the basal cell (Fig. 1-10c). The swelling of the partitioning membranes may increase the interface between the apoplast and symplast. Naidoo and Naidoo (1998b) indicated that the closed end of the partitioning membranes terminate in the cytosol of the basal cell in *S. virginicus*. Paradermal sections also showed that the partitioning membranes are not linked with the plasma membrane in the neck and bottom regions of the basal cell in Rhodes grass (Fig. 1-10b, c). These facts suggest that the partitioning membranes are

linked with the plasma membrane only along the cell wall between the basal and cap cells (Figs. 1-9 and 1-12).

The salt-transport pathway from the vein via the basal cell to the cap cell is not fully clarified. However, several hypotheses on the loading of salts to the basal cell and the transporting to the cap cell have been presented. For the salt loading to the basal cell, Oross *et al*. (1985) proposed that in *C. dactylon* salts are incorporated into the inside of the partitioning membranes from the apoplast of the adjacent mesophyll and epidermal cells via the cell wall of the neck region of the basal cell. The salts are then transported to the cytosol across the partitioning membranes. On the other hand, Naidoo and Naidoo (1998b) suggested that in *S. virginicus* the symplastic continuity between the basal cell and adjacent cells facilitates the salt loading. The occurrence of plasmodesmata between these cells in Rhodes grass supports the salt loading through the symplastic routes (Figs. 1-9a, 1-10c, and 1-12). In addition, the combination of apoplastic and symplastic routes to the basal cell has been suggested (Naidoo and Naidoo 1999). This idea is supported by the fact that intense ATPase activity is detected at the plasma membrane and the partitioning membranes in the basal cell and at the plasmodesmata between the basal and mesophyll cells, in *S. virginicus* (Naidoo and Naidoo 1999; Kobayashi 2008). As for transport from the basal cell to the cap cell, the symplastic route is proposed (Oross *et al*. 1985; Kobayashi 2008). Occurrence of abundant plasmodesmata connecting the basal cell and the cap cell supports the symplastic route (Figs. 1-9a, b and 1-12). In contrast to this symplastic route, Levering and Thomson (1971) proposed the apoplastic route, in which salts are actively incorporated into the inside of the partitioning membranes from the cytosol of the basal cell in *S. foliosa*. The salts are then transported to the apoplast of the cap cell. In addition, Semenova *et al*. (2010) proposed that in *D.*

spicata mechanical compression and expansion of partitioning membranes act to discharge the salt solution into the apoplastic space of the cap cell. However, expansion of partitioning membranes was seen only in the base region of the basal cell in Rhodes grass (Fig. 1-10c).

In any case, the occurrence of abundant mitochondria in the cells constituting the salt gland (Figs. 1-9 and 1-10) suggests that the salt transport is an energy-requiring process (Levering and Thomson 1971; Oross *et al.* 1985; Naidoo and Naidoo 1999; Barhoumi *et al*. 2008; Semenova *et al*. 2010). Preference of ion excretion (Fig. 1-2; Kobayashi *et al*. 2007; Kobayashi and Masaoka 2008) supports active transport across the cell membranes.

The cavity between the cell wall and the cuticle at the top of the cap cell (Figs. 1-9a, c and 1-12) is called ‘cuticular cavity’ or ‘collecting chamber’ (Oross and Thomson 1982a; Naidoo and Naidoo 1998b; Somaru *et al*. 2002; Barhoumi *et al*. 2008). This structure is considered to be an extracellular space to accumulate high-salinity solution. However, the salt-excretion pathway from the cap cell through the cavity to the outside has not been clarified. In the following chapters, I focus on the excretion process from the cap cell to the outside and investigated the surface structures of the cap cell and the excreted droplets.

Figures

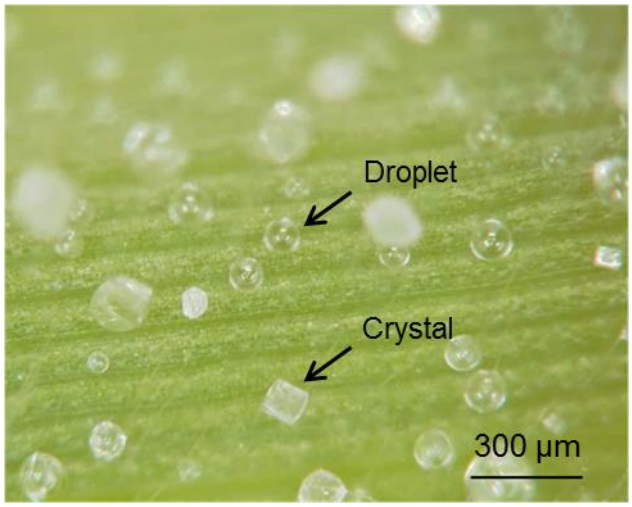

Fig. 1-1

Salty water droplets and crystals on the abaxial leaf surface of Rhodes grass treated with 400 mM NaCl for 7 d. This still image was captured from a video taken with a digital stereomicroscope.

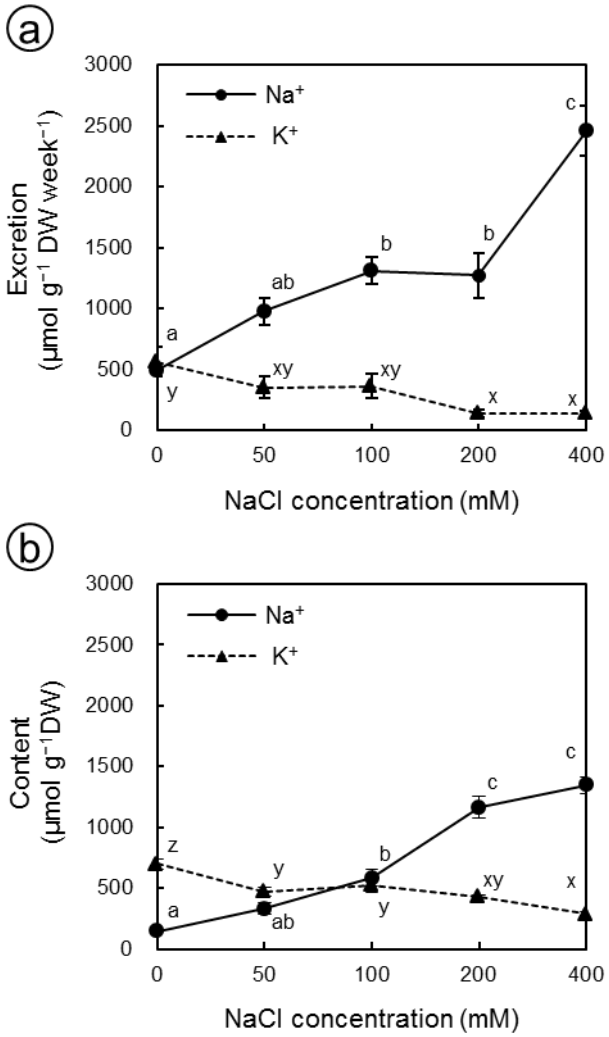

Fig. 1-2

Effects of NaCl treatment on amounts of Na^+ and K^+ excreted on leaf surfaces and contained in the leaf of Rhodes grass. Plants were treated with NaCl (0, 50, 100, 200, or 400 mM) for 14 d. (*a*) Amount excreted on the leaf surfaces for 7 d (from day 8 to 14 of NaCl treatment). (*b*) Content in leaf tissue after 14 d of NaCl treatment. Values are calculated as micromoles per gram of leaf dry weight (DW). The data are means ± SE (n = 4). The same letter above the points indicates no significant difference in each ion ($P < 0.05$).

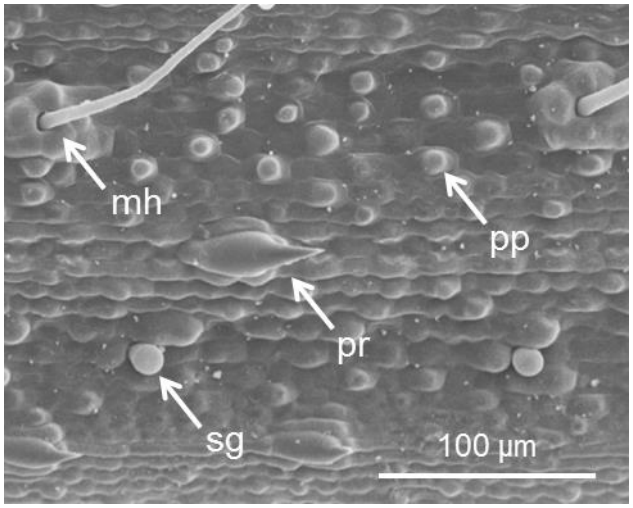

Fig. 1-3

Scanning electron micrograph of the abaxial leaf surface of Rhodes grass without NaCl treatment. Abbreviations: *mh*, macrohair; *pp*, papilla; *pr*, prickles; *sg*, salt gland.

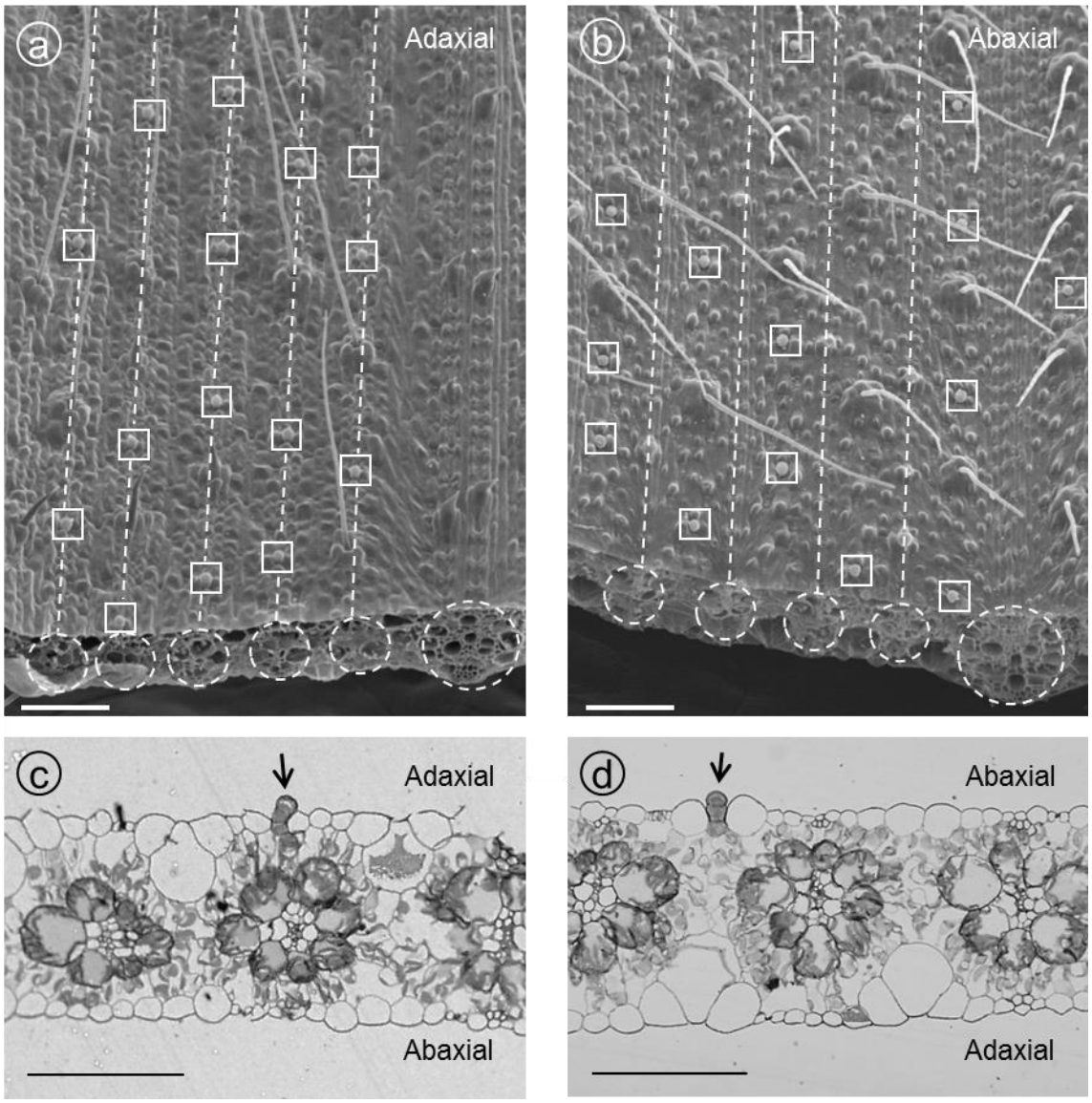

Fig. 1-4

Location of salt glands on the adaxial (*a*, *c*) and the abaxial (*b*, *d*) leaf surfaces of Rhodes grass without NaCl treatment. (*a*, *b*) Inclined views at 45º to the surfaces observed by SEM. Boxes indicate the locations of salt glands. Dashed circles and lines indicate the locations of veins. (*c*, *d*) Transverse sections stained with toluidine blue and observed by light microscopy. Arrows indicate salt glands. Bars show 100 μm for all panels.

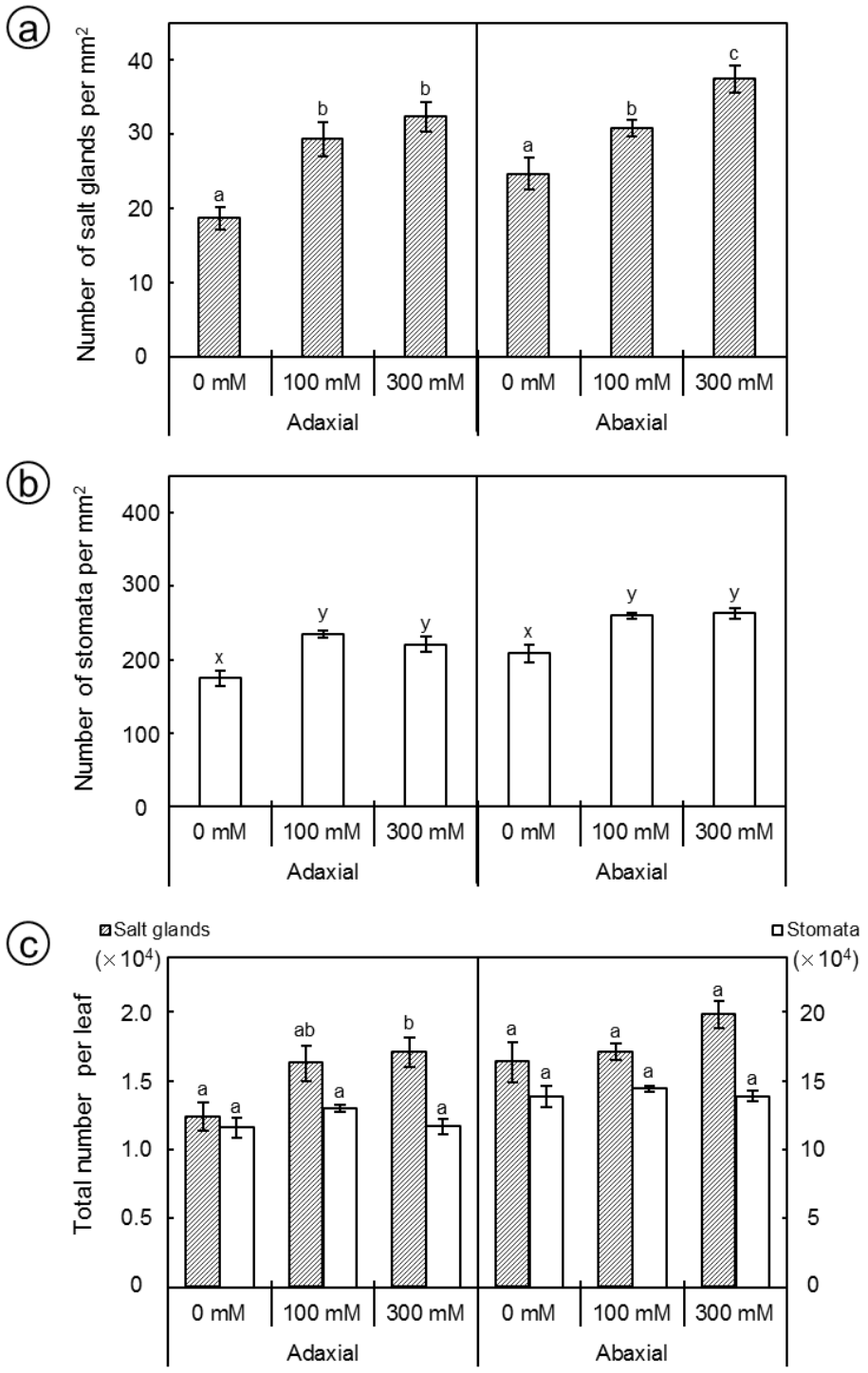

Fig. 1-5

Effects of NaCl treatment on the number of salt glands and stomata on the adaxial and abaxial leaf surfaces of Rhodes grass. Plants were treated with NaCl (0, 100, or 300 mM) for 14 d. (*a*) Salt gland density [number per unit of leaf area (1 mm^2)]. (*b*) Stomatal density [number per unit of leaf area (1 mm^2)]. (*c*) Total number of salt glands and stomata per leaf. Data are means ± SE from 12 micrographs (4 areas in 3 individuals). The same letter above the bars indicates no significant difference in each surface ($P < 0.05$).

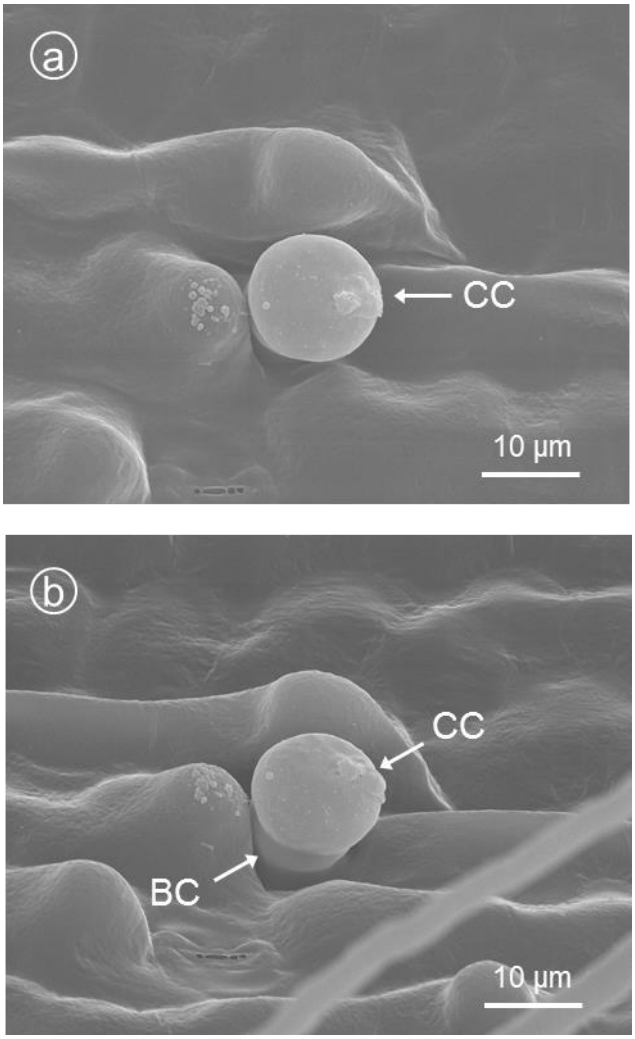

Fig. 1-6

Stereoscopic view by SEM of a salt gland on the abaxial leaf surface of Rhodes grass without NaCl treatment. (*a*) Top view of the leaf surface. (*b*) Inclined view at 45º to the leaf surface. Abbreviations: *BC*, basal cell; *CC*, cap cell.

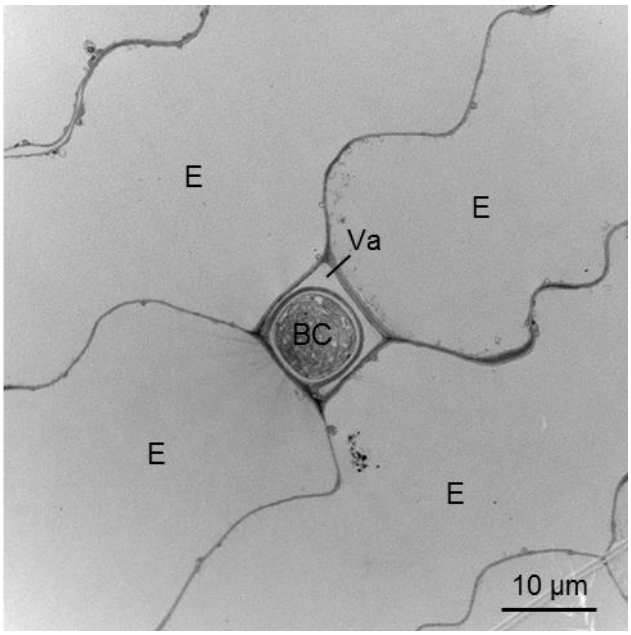

Fig. 1-7

Paradermal view by TEM of a leaf of Rhodes grass with a neck region of basal cell. Abbreviations: *BC*, basal cell; *E*, epidermal cell; *Va*, vallecula.

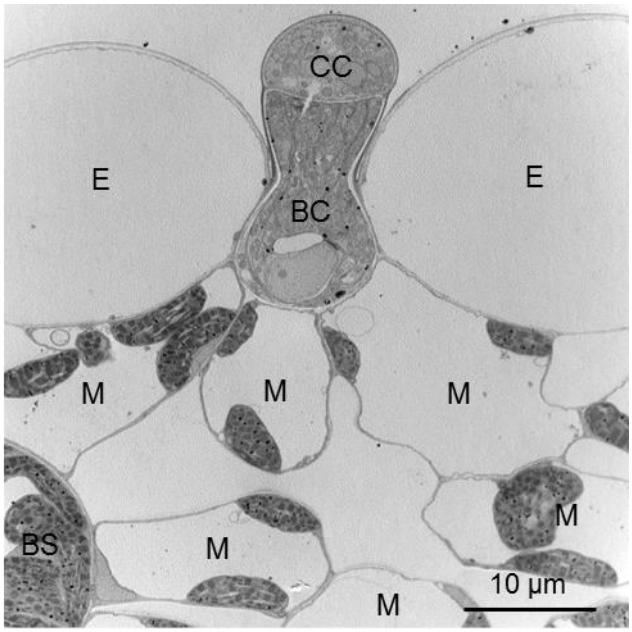

Fig. 1-8

Longitudinal view by TEM of a leaf of Rhodes grass with a salt gland. Abbreviations: *BC*, basal cell; *BS*, bundle sheath cell; *CC*, cap cell; *E*, epidermal cell; *M*, mesophyll cell.

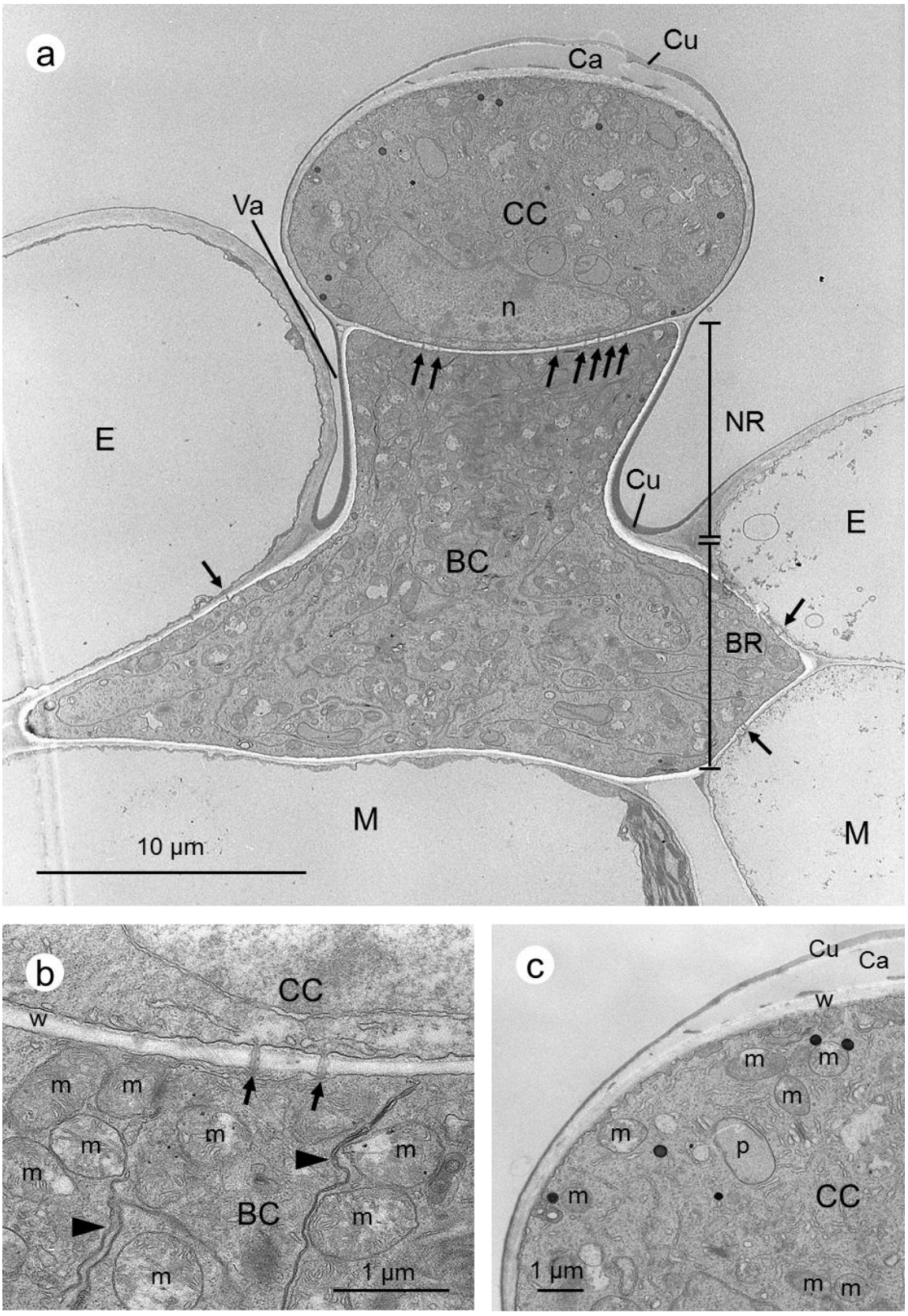

Fig. 1-9 (*see next page*)

Fig. 1-9 (*see previous page*)

Longitudinal view by TEM of a salt gland of Rhodes grass without NaCl treatment. (*a*) Overall view of a salt gland. (*b*) Enlarged view of the connecting region between the basal and cap cells. (*c*) Enlarged view of a part of the cap cell. Abbreviations: *BC*, basal cell; *BR*, base region of basal cell; *Ca*, cavity; *CC*, cap cell; *Cu*, cuticle; *E*, epidermal cell; *M*, mesophyll cell; *m*, mitochondrion; *n*, nucleus; *NR*, neck region of basal cell; *p*, undeveloped plastid; *Va*, valleculae; *w*, cell wall. Arrows indicate plasmodesmata, and arrowheads indicate partitioning membranes.

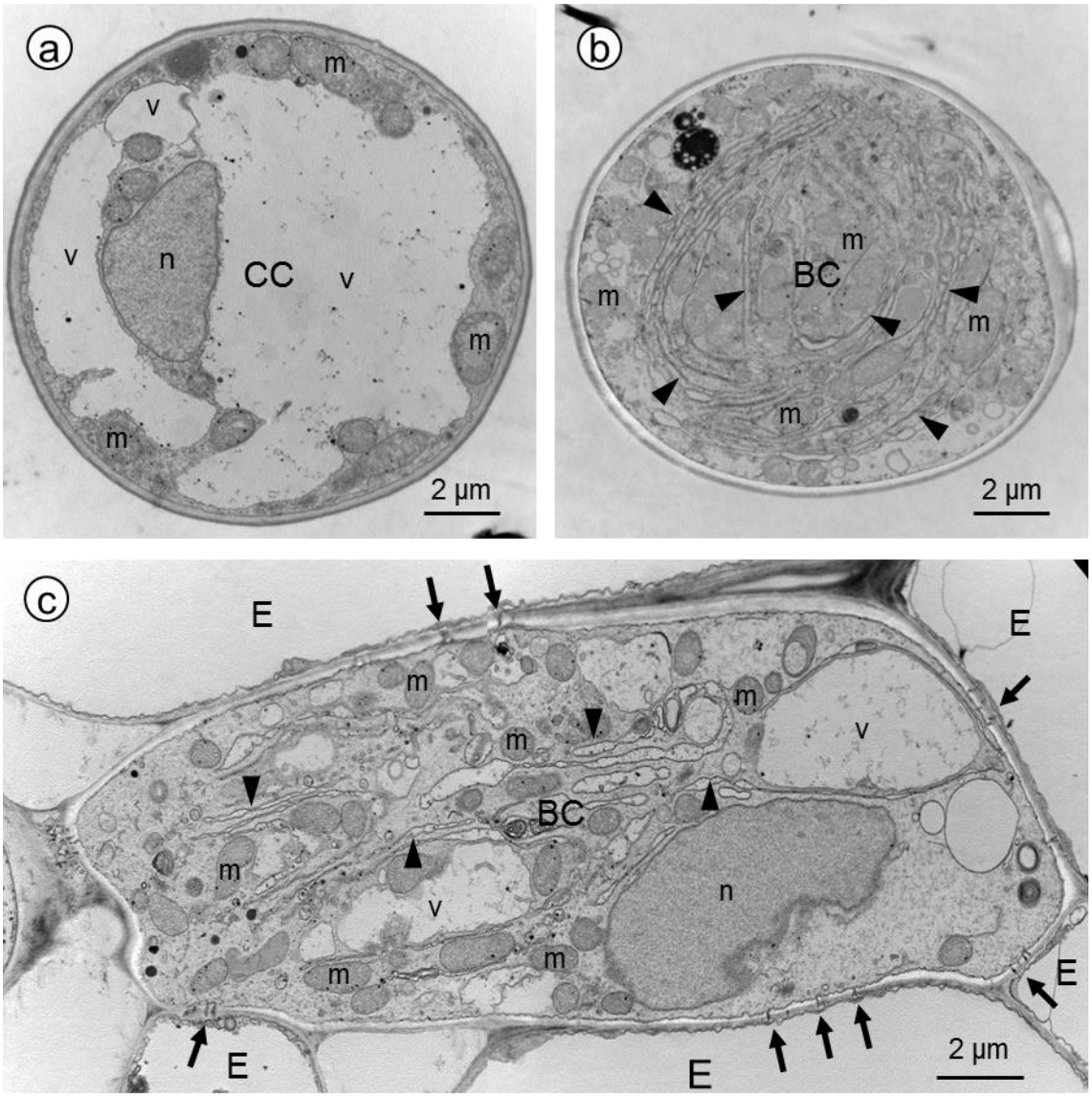

Fig. 1-10

Paradermal views of salt glands of Rhodes grass without NaCl treatment. (*a*) Cap cell. (*b*) Neck region of basal cell. (*c*) Base region of basal cell. Abbreviations: *BC*, basal cell; *CC*, cap cell; *E*, epidermal cell; *m*, mitochondrion; *n*, nucleus; *v*, small vacuole. Arrows indicate plasmodesmata, and arrowheads indicate partitioning membranes.

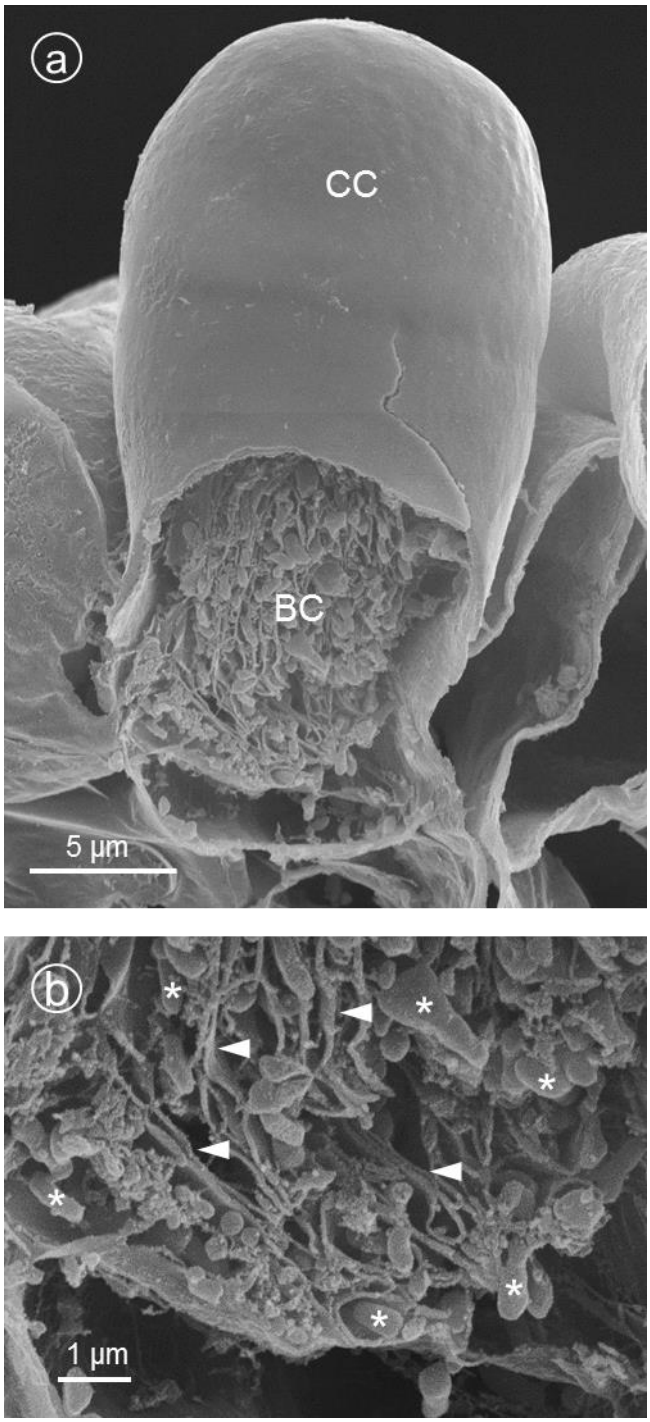

Fig. 1-11

Scanning electron micrographs of a salt gland on the freeze-cracked leaf of Rhodes grass. (*a*) Overall view of a salt gland with a smooth globular cap cell and a basal cell cracked partly. (*b*) Enlarged view of the cracked region of the basal cell. Abbreviations: *BC*, basal cell; *CC*, cap cell. Arrowheads indicate partitioning membranes, and asterisks indicate mitochondria.

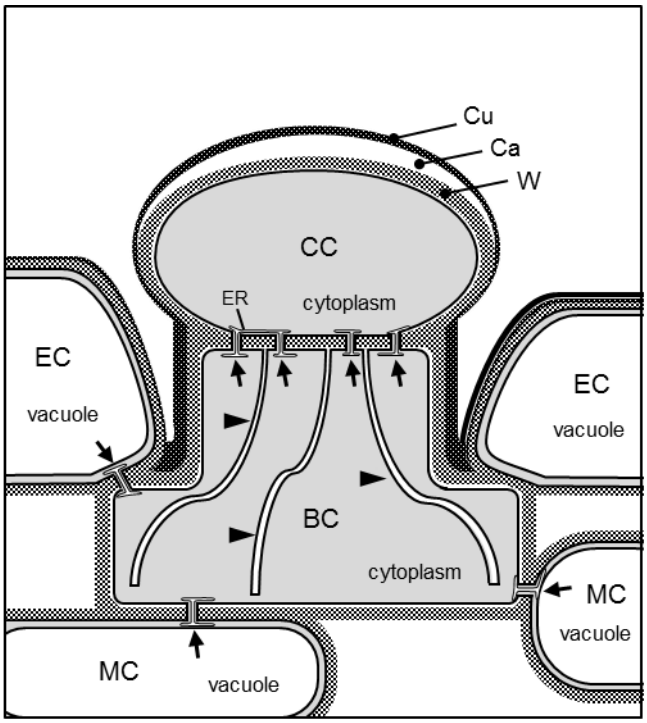

Fig. 1-12

A schematic explanation of the longitudinal view of a salt gland. Abbreviations: *BC*, basal cell; *Ca*, cavity; *CC*, cap cell; *Cu*, cuticle; *EC*, epidermal cell; *ER*, endoplasmic reticulum; *MC*, mesophyll cell; *W*, cell wall. Arrows indicate plasmodesmata, and arrowheads indicate partitioning membranes.

Chapter 2

Salt excretion from the salt glands in Rhodes grass as evidenced by low-vacuum scanning electron microscopy

The contents were published in Oi *et al*. (2013) *Flora* 208: 52–57.

http://dx.doi.org/10.1016/j.flora.2012.12.006

Introduction

The bicellular salt glands in the Poaceae have been postulated to excrete salts in the previous studies. However, clear evidence for this phenomenon has not been presented yet. Salt excretion on the leaf surfaces is readily detectable using a light microscope, either as salt crystals or as water droplets (Liphschitz *et al*. 1974; Chapter 1). However, it is difficult to observe the excretion products from the salt glands by electron microscopy. Soluble attachments on the leaf surface are completely removed during specimen preparation for conventional electron microscopy, such as fixation, dehydration, and drying. Although previous studies by SEM showed salt crystals on the leaf surfaces in the Poaceae (Liphschitz *et al*. 1974; Amarasinghe and Watson 1989; Somaru *et al*. 2002; Barhoumi *et al*. 2007), the relation of excreted salts and salt glands has not been shown. Amarasinghe and Watson (1989) emphasized that SEM was necessary to show the association between salt crystals and salt glands. However, at the electron-microscopic level clear evidence is still missing for salt excretion by these bicellular salt glands.

In this chapter, I determined whether the bicellular salt glands actually excrete salts in Rhodes grass. To examine the excreted materials, I observed leaves of Rhodes grass by SEM in a low-vacuum mode (LV-SEM), which allows observing specimens without preparation procedures. In addition, I confirmed by energy dispersive X-ray spectrometry (EDS) that the excreted materials indeed contain alkali metal ions and chloride ions.

Materials and Methods

Plant growth conditions and salt treatment

Caryopses of Rhodes grass (*Chloris gayana* Kunth 'Katambora') were germinated on culture soil in 500-mL pots in a growth chamber. The cultivation condition was controlled at 30°C/25°C (light/dark), relative humidity of 60%, 14-h photoperiod, and light intensity of 500 μmol m^{-2} s^{-1}. Following germination, two seedlings per pot were left by thinning and were grown with tap water. After 7 d of growth, salt treatment was conducted by supplying 150 mL of 100 mM NaCl solution every other day for 14 d. After the treatment, the sixth leaves were used for observations. The sixth leaves had not appeared at the beginning of the NaCl treatment and fully expanded at 7 d of the treatment.

Low-vacuum SEM (LV-SEM) observation

To observe salt excretion on the leaf surfaces, fresh segments of the sixth leaves of Rhodes grass were used after the plants were treated with NaCl treatment for 14 d. Small segments (approx. 3 mm × 5 mm) were excised from the middle portion of the leaf blades and were mounted on a stub with adhesive carbon tape. The specimens were immediately observed with a scanning electron microscope (S-3000N, Hitachi) equipped with a cool stage, in a low-vacuum mode (30 Pa) at −5°C and at 15 kV accelerating voltage. The back-scattered electron (BSE) images were obtained in the composition (COMPO) mode.

The leaf segments mounted on a stub were washed with running tap water for 30 s, rinsed with distilled water three times, and dried with a blower for 30 s after the excess

water was absorbed with paper towels. Washed leaf surfaces were also observed with the scanning electron microscope under the same conditions.

The numbers of globular materials observed on the unwashed leaves and of the salt glands observed on the washed leaves were counted on scanning electron micrographs at 100-fold magnification (an area of 1.11 mm^2). The micrographs were taken from four separate fields on each leaf surface except the midrib and blade margins, and the average of counts on four micrographs was considered as one replicate. The density [number per unit of leaf area (1 mm^2)] of the globular materials and the salt glands was statistically compared by paired *t*-test (n = 4) using SPSS 14.0 for Windows.

Energy dispersive X-ray spectrometry (EDS)

To analyse the chemical elements in the excreted materials on the leaf surfaces, fresh segments of the sixth leaves of Rhodes grass were used at the end of a NaCl treatment for 5 d. Small segments (approx. 3 mm × 5 mm) were excised from the middle portion of the leaf blades and were mounted on a stub with adhesive carbon tape. The specimens were analysed with a low-vacuum scanning electron microscope (TM-1000, Hitachi) at 5 Pa equipped with an EDS system (SwiftED1000, Oxford Instruments, Abingdon, UK). Spot analyses with a diameter of approximately 100 nm were performed. During the measurements accelerating voltage was 15 kV, working distance was 4.9–5.5 mm, and the counts were collected for 100 s.

Conventional SEM observation

To observe the surface of the cap cell of the salt glands at high magnification, the tenth leaves of Rhodes grass were used at the end of NaCl treatment for 14 d. Small

segments of leaves were fixed in glutaraldehyde, dehydrated in ethanol, critical-point dried in CO_2, and then coated with gold, as described in chapter 1. The specimens were then examined with a scanning electron microscope (S-4200K, Hitachi) at an accelerating voltage of 15 kV.

SEM observation with freeze cracking

To observe the structure under the surface of the cap cell three-dimensionally, freeze cracked leaves were observed by SEM. Specimens were prepared from the sixth leaves of Rhodes grass grown for 21 d without NaCl treatment. The leaf segments were fixed, freeze-cracked, dehydrated, dried, coated with gold, and then observed with a scanning electron microscope (S-4200K, Hitachi), as described in chapter 1.

Results

Globular materials were observed on the unwashed leaf surfaces of both control and NaCl-treated plants (Figs. 2-1a, b and 2-2a, b). The diameter of the globular materials was 40–80 μm. The globular materials and the macrohairs were distributed on the same lines, parallel with veins. Salt glands were hardly observed in the unwashed leaf surfaces. Angular deposits of high brightness were often observed in the globular materials. These deposits were often protruding from the globular materials and were more prominent on the NaCl-treated plants than on the control plants (Figs. 2-1a, b and 2-2a, b).

The globular materials became removed by washing the leaves with water (Figs. 2-1c, d and 2-2c, d). Then, salt glands were clearly visible on the washed leaf surfaces.

The head of a salt gland, the cap cell, was smooth and globular in shape, and its diameter was approximately 15 μm. (Figs. 2-1d and 2-2d). Distribution of the salt glands and the macrohairs followed the same lines, parallel with veins. Shape and size of salt glands on the washed leaf surfaces were not much different between the NaCl-treated plants and the control plants (Figs. 2-1d and 2-2d).

Rows of silica cells were always observed on the leaf surfaces, regardless of NaCl treatment or leaf washing (Figs. 2-1a, c and 2-2a, c). These cells accumulate silica (Soni *et al*. 1972), and the accumulations appear bright in BSE images in the COMPO mode of SEM (Dietrich *et al*. 2003). The outlines of the silica cells are shown in enlarged views (Figs. 2-1b, d and 2-2b, d).

To verify that the globular materials were derived from the salt glands, I estimated their density. The densities were almost equal between the globular materials observed on the unwashed leaves and the salt glands observed on the washed leaves, in both control and NaCl-treated plants (Fig. 2-3).

Leaf surface structures got damaged within a few minutes during the observation by LV-SEM. The cap cells of salt glands were smooth and globular at first (Fig. 2-4a), but became partly crushed after a few minutes, showing then dented appearances (Fig. 2-4b). Conventional SEM observation at high magnification (1500×) showed the surface structure of these salt glands in detail (Fig. 2-5): the cap cell of the salt gland has a smooth surface, without any pores or rupturing scars on the cuticle.

The chemical elements in the excreted materials and on the leaf surfaces were examined by spot analysis of EDS (Fig. 2-6). In the control plant samples, the spectrum of the excreted material showed the peak of potassium (Fig. 2-6a). In the NaCl-treated plants, the spectrum of the excreted materials showed the peaks of sodium and chlorine

in addition to potassium (Fig. 2-6b). Spectra of leaf surface areas without excreted materials did not show such sharp peaks in both control and NaCl-treated plants (Fig. 2-6c, d)

In the specimens prepared by the freeze cracking method, the three-dimensional ultrastructure of the cap cell of the salt gland was clearly observed (Fig. 2-7). The cap cell is located above the basal cell, which constitutes the lower part of the salt gland. At the top of the cap cell, the cuticle is separated from the cell wall, so that a cavity is formed (Fig. 2-7 *Ca*).

Discussion

Leaves of Rhodes grass excrete water droplets on their surfaces (Chapter 1). Supposedly, these droplets are excreted from the salt glands. However, no direct evidence has been presented showing that the salt glands really excrete these droplets. In this chapter, I attempted to confirm the salt excretion via the glands by LV-SEM observation, which allows to observe fresh materials without conventional preparation procedures and thus makes possible observation of excreted materials. LV-SEM observation reveals that the globular materials on the unwashed leaf surfaces are positioned on the same lines as the macrohairs, between the leaf veins (Figs. 2-1a and 2-2a). On the other hand, by this approach salt glands were hardly observed on the unwashed leaf surfaces. However, the glands became clearly visible after washing the leaf surfaces and were distributed on the same lines as the macrohairs in common with the globular materials, which disappeared due to washing of the leaf surfaces (Figs. 2-1c and 2-2c; Chapter 1). The density of these globular structures on the unwashed leaf

surfaces corresponds to that of the salt glands seen at washed surfaces in both control and NaCl-treated plants (Fig. 2-3). These findings suggest that the globular materials correspond to the water droplets under the light microscope and that the salt glands indeed excrete droplets just above their cap cells.

Angular deposits of high brightness in the globular materials were probably crystals of salt forming in the excreted water. EDS analyses give evidence that the globular materials at the unwashed leaf surfaces contained sodium, chlorine, and potassium, whereas these elements were not detected on the area without the globular materials (Fig. 2-6). The count of sodium and chlorine was more pronounced in the globular materials of the NaCl-treated plant than in that of the control plant. These findings indicate that higher sodium and chlorine content in the globular materials resulted from NaCl treatments of the plants and suggest that these ions had been excreted after passing the plant tissues. As described in chapter 1, ion analysis indicated that the amount of sodium excreted on the leaf surfaces of Rhodes grass increased with increased NaCl concentrations in the growing substrate. In both control and NaCl-treated plants, the globular materials contained potassium (Fig. 2-6a, b). Such excretion of potassium was reported in the previous studies (Kobayashi *et al*. 2007; Chapter 1). The potassium was probably taken up by the plants from the fertilizer in the soil where they were growing. These findings indicate that the salt glands on leaves of Rhodes grass excrete sodium and chlorine under saline conditions in addition to potassium.

The cavity between the cell wall and the cuticle at the top of the cap cell was observed three-dimensionally (Fig. 2-7 *Ca*). Such cavities have been observed on several Poaceae plants by TEM and are called ‘cuticular cavity’ or ‘collecting chamber’

(Oross and Thomson 1982a; Naidoo and Naidoo 1998b; Somaru *et al*. 2002; Barhoumi *et al*. 2008; Chapter 1). This compartment is considered to be an extracellular space where a highly concentrated saline solution accumulates temporarily before excretion through the cuticle occurs (Chapter 1). Kobayashi (2008) reviewed the pertinent literature and suggested that a continuous accumulation of salts may increase the hydrostatic pressure of the solution in the cavity, so that the cuticle becomes stretched and finally is ruptured at pre-existing weak spots in the cuticle, thereby allowing the solution to escape. Also Barhoumi *et al*. (2008) investigating *A. littoralis* (Poaceae) suggested that the high salt accumulation in the cavity probably increases the hydrostatic pressure and finally brings about the cavity to burst. Rupture of the cuticle and release of the accumulating saline solution was assumed to be the end of functioning of an individual salt gland.

In the present study, excreted materials existed on most of the salt glands on the unwashed leaves, and cap cells of the salt glands on the washed leaves had a smooth and globular appearance without signs of ruptures of the cuticle (Figs. 2-1 and 2-2). Rupture of the cuticle was not observed, even at high magnification (Fig. 2-5). This indicates that the salt glands of Rhodes grass excrete salts without rupturing their cuticle. Although dented salt glands were also observed, these can be interpreted as artefacts from electron-beam damages or vacuum effects (Fig. 2-4). Also in Rhodes grass, the cuticle on the top of the cap cell may be vulnerable because of the lack of physical support by the cell wall (Fig. 2-7 *Cu*). In addition to ruptures, porous structures were not observed at the surfaces of the cap cells (Figs. 2-1d, 2-2d, 2-4a, and 2-5). Nevertheless, the cuticle may have minute openings allowing the salts to pass, and these openings could be observed at higher magnification on more intact specimens. Pathan *et al*.

(2008) succeeded in observing the wax microstructures on the salt gland cuticle of *Chenopodium* (dicotyledon) by SEM on air-dried specimens. Use of such an air-drying technique or of cryo-SEM possibly also in Rhodes grass could visualize the detailed cuticle structure of the salt glands.

Present observations on the salt glands of Rhodes grass suggest that the saline solution accumulated in the cavity at the top of the cap cell leaks out without rupturing of the cuticle. In the following chapter, I investigated the surface microstructure of the cuticle of the cap cell and discuss the salt-excretion process through the cuticle in more detail.

Figures

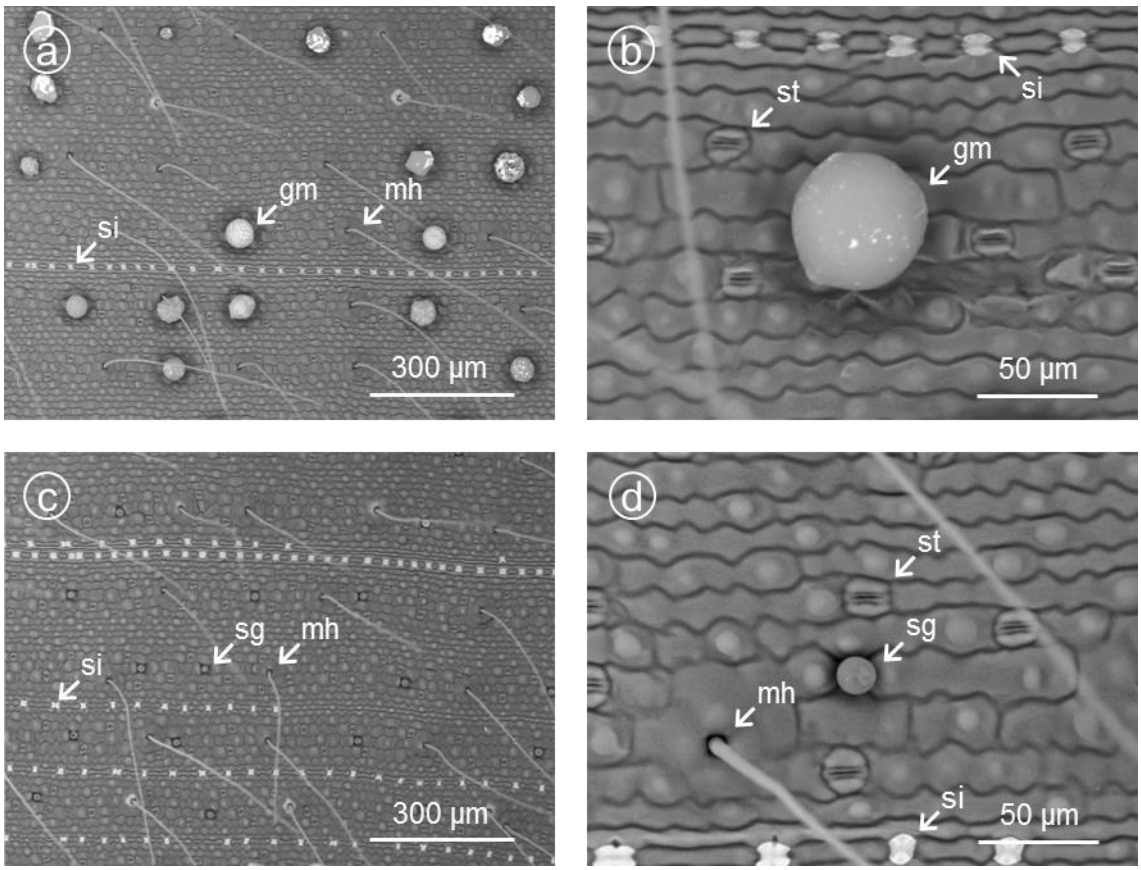

Fig. 2-1.

Abaxial leaf surfaces of Rhodes grass without NaCl treatment (controls). The leaf surfaces were observed by LV-SEM. (*a*, *b*) Unwashed leaves. (*c*, *d*) Washed leaves. Abbreviations: *gm*, globular material; *mh*, macrohair; *sg*, salt gland; *si*, silica cell; *st*, stoma.

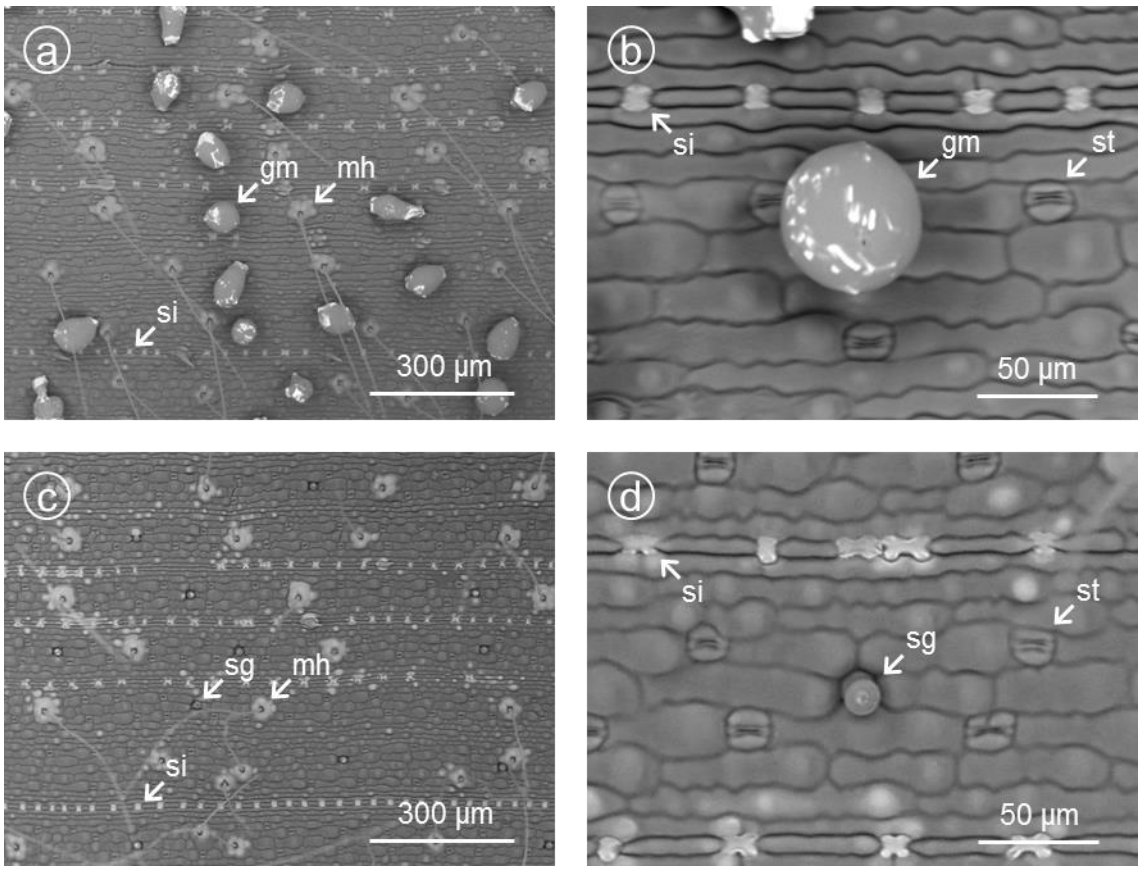

Fig. 2-2.

Abaxial leaf surfaces of Rhodes grass treated with 100 mM NaCl for 14 d. The leaf surfaces were observed by LV-SEM. (*a*, *b*) Unwashed leaves. (*c*, *d*) Washed leaves. Abbreviations: *gm*, globular material; *mh*, macrohair; *sg*, salt gland; *si*, silica cell; *st*, stoma.

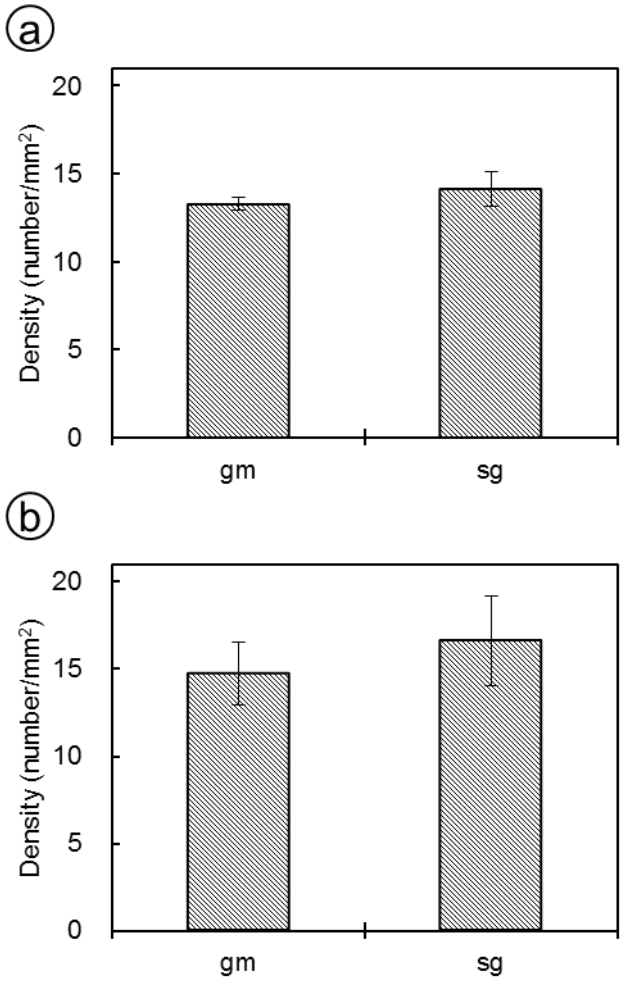

Fig. 2-3.

The density [number per unit of leaf area (1 mm^2)] of the globular materials (*gm*) observed on the unwashed leaves and of the salt glands (*sg*) observed on the washed leaves, on the abaxial surfaces of Rhodes grass. (*a*) Control. (*b*) Plants treated with 100 mM NaCl for 14 d. Data are means ± SE (n = 4). There were no significant differences between the densities of the globular materials and the salt glands, both in control (P = 0.31) and in NaCl-treated plants (P = 0.43).

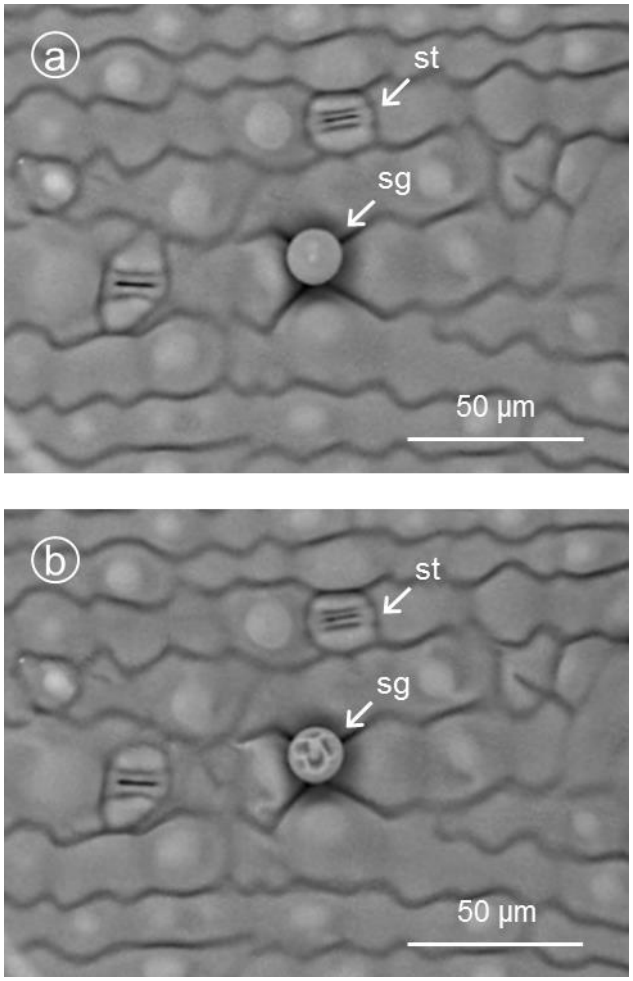

Fig. 2-4.

Washed abaxial leaf surface of Rhodes grass without NaCl treatment (controls). The leaf surface was observed by LV-SEM. (*a*) First image. (*b*) Second image captured a few minutes after the first one showing lesions at the top of a salt gland. Abbreviations: *sg*, salt gland; *st*, stoma.

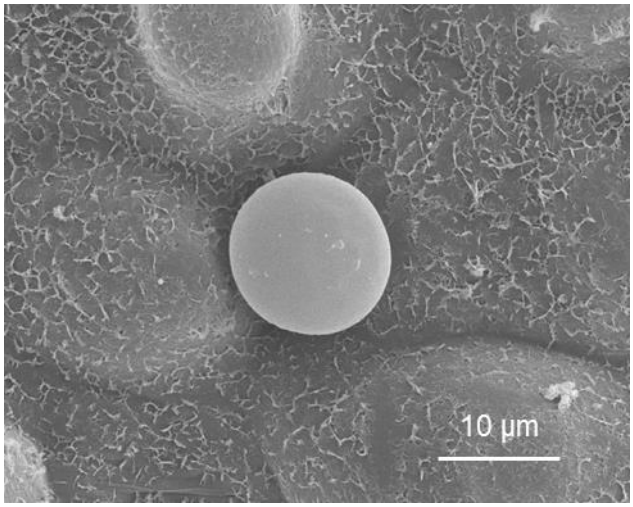

Fig. 2-5.

A cap cell of a salt gland on the abaxial leaf surface of Rhodes grass treated with 100 mM NaCl for 14 d and observed by conventional SEM. The specimen was fixed, dehydrated, critical point dried, and coated with gold.

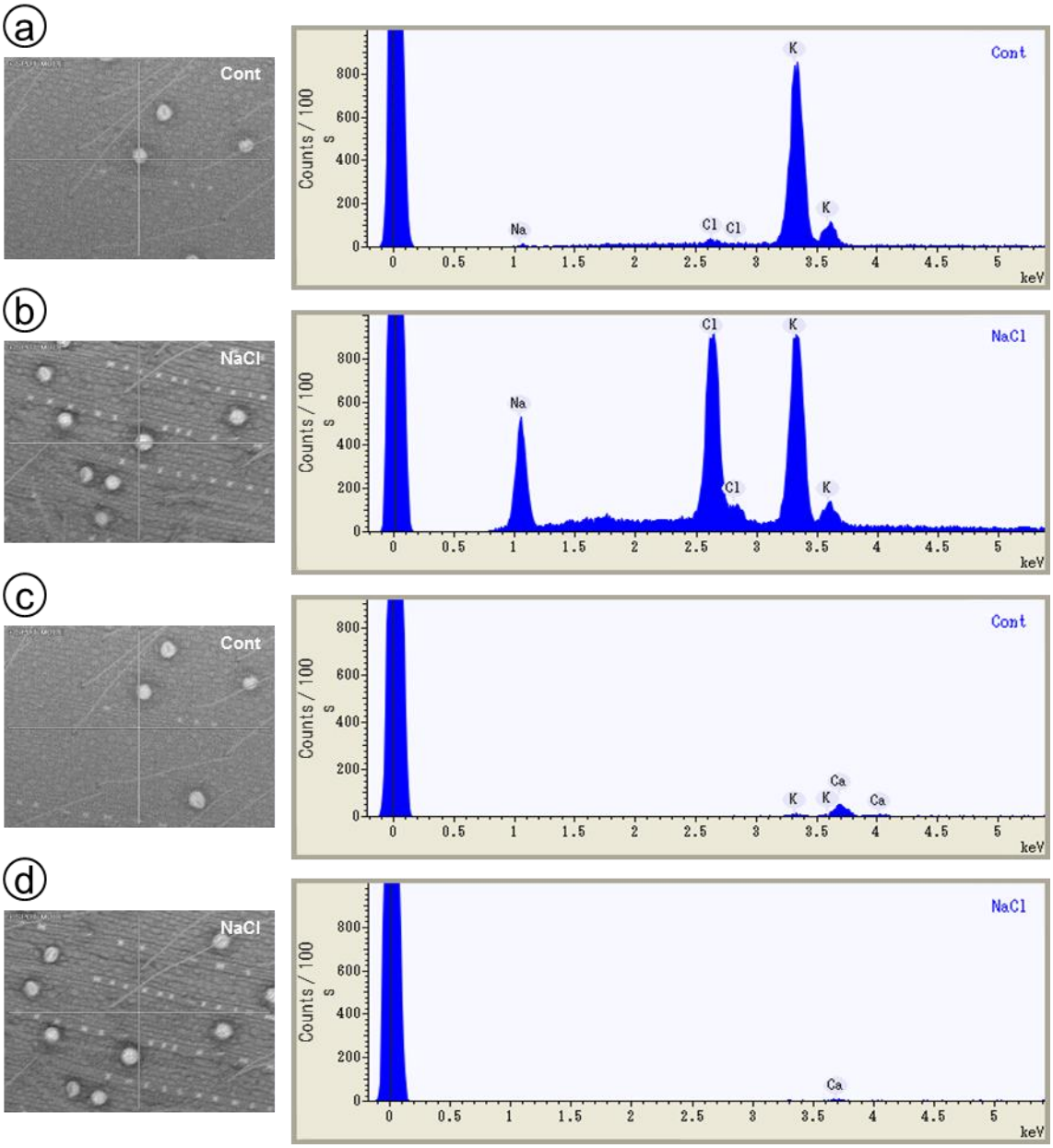

Fig. 2-6.

Scanning electron micrographs (*left*) for spot analysis of EDS, and X-ray spectra (*right*) on the unwashed abaxial leaf surfaces of Rhodes grass. Location of the spot analysis is indicated by the intersection of lines on the scanning electron micrograph. The large peak on the left in each spectrum is background noise. (*a*, *b*) Analysis was made on the excreted material. (*c*, *d*) Analysis was made on the leaf surface without excreted material. (*a*, *c*) Control. (*b*, *d*) Plant treated with 100 mM NaCl for 5 d. Counts were collected for 100 s.

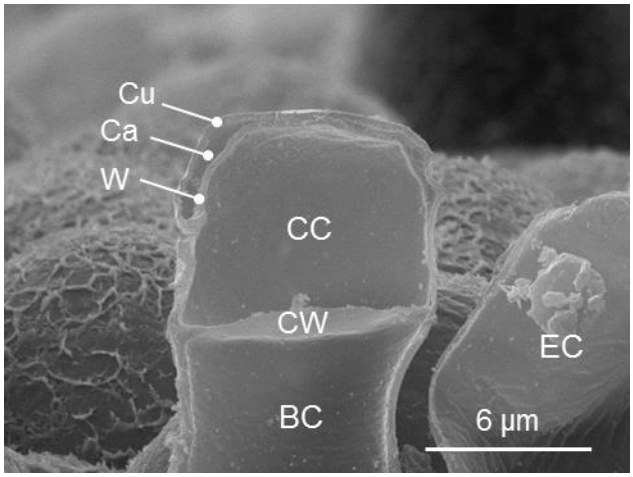

Fig. 2-7.

A salt gland of Rhodes grass that was frozen and cracked longitudinally. Abbreviations: *BC*, basal cell; *Ca*, cavity; *CC*, cap cell; *Cu*, cuticle; *CW*, common cell walls between basal and cap cells; *EC*, epidermal cell; *W*, cell wall.

Chapter 3

Salt excretion through the cuticle without disintegration of fine structures in the salt glands of Rhodes grass

The contents will be published in Oi *et al*. (2014) *Flora* 209.

http://dx.doi.org/10.1016/j.flora.2014.02.004

Introduction

In chapter 1, I studied the distribution and morphology of salt glands of Rhodes grass by SEM on the leaf specimens processed by chemical fixation and critical-point drying. The salt glands of Rhodes grass are distributed above the small veins on the adaxial surface and between the veins on the abaxial surface. The cap cell of a salt gland is smooth and globular in shape, and its diameter is approximately 15 μm. In chapter 2, I examined droplets excreted from the salt glands by LV-SEM. LV-SEM allows observing fresh hydrated specimens without chemical fixation and critical-point drying, and thus makes possible observation of soluble attachments on the specimen surfaces. LV-SEM observation of fresh leaves in Rhodes grass showed that the bicellular glands really excrete droplets.

My observations by SEM and LV-SEM showed that there is no rupturing scar or porous structure at the surfaces of the cap cells. However, there is a possibility that these techniques cannot detect minute openings or preserve fine structures on the specimen surfaces. It was reported that LV-SEM observation reduces the resolution and stability of specimens at high magnification (Pathan *et al*. 2008). On the other hand, surface fine structures might be damaged during specimen preparation by conventional SEM (Pathan *et al*. 2008). To clarify the salt-excretion process through bicellular salt glands in Rhodes grass, it is necessary to observe the surfaces of the structurally-intact glands at higher magnification.

Cryo-SEM (low-temperature SEM) is considered to be superior to conventional SEM or LV-SEM in the preservation of plant surface details (Jørgensen *et al*. 1995; Pathan *et al*. 2008; Read and Jeffree 1991). It is a method for observing frozen-hydrated specimens at low temperature in the scanning electron microscope (Read and Jeffree

1991). Cryofixation is more rapid and less damaging than chemical fixation, and cryo-SEM can visualise with higher resolution than LV-SEM.

In this chapter, I used cryo-SEM to reveal the fine surface structures of the salt glands in Rhodes grass and discuss the excretion process of the salt-containing water through the cuticle of the cap cell.

Materials and Methods

Plant growth conditions and salt treatment

Caryopses of Rhodes grass (*Chloris gayana* Kunth 'Katambora') were germinated on culture soil in 500-mL pots in a growth chamber. The cultivation condition was controlled at 28°C/20°C (light/dark), relative humidity of 60%, 14-h photoperiod, and light intensity of 500 μmol m^{-2} s^{-1}. Following germination, two seedlings per pot were left by thinning and were grown with tap water. After 7 d of growth, salt treatment was conducted by supplying 150 mL of 100 mM NaCl solution every other day for 14 d. After the treatment, the seventh leaves were used for observations. The seventh leaves had not appeared at the beginning of NaCl treatment and fully expanded at 7 d of the treatment.

Cryo-SEM observation

Small segments (approx. 3 mm × 5 mm) were excised from the middle portion of the leaf blades and were mounted on a stub with adhesive carbon tape; the margins of the segments were pressed tightly to the tape with tweezers. The specimens were immersed in liquid nitrogen (−196°C) for cryo-fixation and were immediately

transferred to a field emission scanning electron microscope (S-4200K, Hitachi) equipped with a cryo-stage (−150°C to −120°C). The surfaces of the specimens without a metal coating were observed, at accelerating voltage of 15 kV for low magnification (under 1000×) or 3 kV for high magnification (at 1000× and over).

To remove excreted materials on the leaf surfaces, the leaves were washed with running tap water for 30 s and were rinsed with distilled water three times. After the excess water was absorbed with paper towels, washed leaves were also cryo-fixed and observed by cryo-SEM as described above.

Other observations

The leaves of Rhodes grass were also examined by conventional SEM to compare with the surface fine structures in cryo-SEM. Small segments of the leaves were fixed in glutaraldehyde, dehydrated in ethanol, critical-point dried in CO_2, and then coated with gold, as described in chapter 1. The specimens were observed with a field emission scanning electron microscope (S-4200K, Hitachi) equipped with a standard specimen stage at 15 kV accelerating voltage.

To confirm the continuous excretion by the salt glands, the fresh leaves of Rhodes grass were examined with a digital microscope (VHX-1000, Keyence, Osaka, Japan) on the identical leaf surface before and after washing the leaf. The leaf sheathes were cut at 20 mm from the base of leaf blades, and the cut ends were immersed in distilled water in 10-mL flasks. The detached leaves were taped to the specimen stage of the digital microscope, and the observation was conducted on the adaxial surfaces of the middle portion of the leaf blades. The leaves were then washed with running tap water for 30 s

and were rinsed with distilled water three times. After the excess water was absorbed with paper towels, the washed leaves were observed again with the digital microscope.

Results

Excreted droplets were observed on the unwashed leaf surfaces by cryo-SEM (Fig. 3-1a, b). These droplets were globular, and their diameters were 75 ± 20 μm. The droplets and the macrohairs were distributed on the same lines, parallel with veins. Salt glands were hardly observed on the unwashed leaf surfaces. The droplets were removed by washing the leaves with water, so that the salt glands were visible on the washed leaf surfaces (Fig. 3-1c, d). The head of a salt gland, the cap cell, was globular in shape, and its diameter was approximately 15 μm (Figs. 3-1d and 3-2b). The salt glands on the washed leaves showed the same distribution as the droplets on the unwashed leaves: the glands were positioned on lines parallel with veins along which macrohairs were also distributed. Droplets and salt glands on the leaves of Rhodes grass without NaCl-treatment were not much different in shape and size from those of the NaCl-treated plants (*data not shown*). Although the droplets on the salt glands disappeared from leaf surfaces just after the washing (Fig. 3-1c, d), they appeared again on the salt glands after 24 h (Fig. 3-1e, f). These droplets covered almost all of the salt glands and their diameters were 25 ± 5 μm.

Cryo-SEM observation at low electron dose (3 kV accelerating voltage) showed the surface fine structures of the leaves in detail (Fig. 3-2a, b, c). Cap cells of the salt glands have smooth surfaces, without any pores or rupturing scars on the cuticle (Fig. 3-2b). Surfaces of epidermal cells were covered with microstructures of epicuticular

waxes (Fig. 3-2a, c). In contrast, the surfaces of the cap cells were smooth and lacked the wax structures (Fig. 3-2b). Conventional SEM observation did not show the wax microstructures on entire leaf surfaces, even on the epidermal cells (Fig. 3-2d). Cryo-SEM was able to observe fine surface structures on the leaves better than conventional SEM.

To elucidate the positional relation between the droplets and the salt glands, unwashed leaf surfaces were observed from an angle. Most of the salt glands were completely hidden under the droplets (average diameter: 75 μm) and were not seen on the leaves of Rhodes grass grown for three weeks (*data not shown*). Instead, the salt glands under the droplets were seen on the leaves of Rhodes grass grown for two weeks (Fig. 3-3). The droplets (average diameter: 45 μm) were spherical and did not spread onto the surfaces of the epidermal cells (Fig. 3-3a, b). An enlarged view showed that the droplet covered the upper region of the cap cell (Fig. 3-3c). Another view showed that the droplet contacted the top of the papilla of the epidermal cell (Fig. 3-3d).

On the washed leaf surfaces, the droplets were observed again on the salt glands 24 h after the leaf washing (Fig. 3-1e, f). To confirm the continuous excretion, identical leaf surfaces of Rhodes grass were observed with a digital microscope for 6 h after washing (Fig. 3-4). Large droplets (diameter: 75 ± 20 μm) were retained on the leaves before washing (Fig. 3-4a), and they disappeared from leaf surfaces completely just after the washing (Fig. 3-4b). Later, droplets were observed again on leaves, and their size increased gradually: the diameters were 20 ± 5 μm at 3 h later (Fig. 3-4c) and 30 ± 5 μm at 6 h later (Fig. 3-4d).

Discussion

Leaves of Rhodes grass excrete droplets on their surfaces (Chapter 1), and these droplets are observed as globular material by LV-SEM (Chapter 2). The LV-SEM observation on unwashed and washed leaves indicates that the droplets are located on the salt glands, which are distributed on lines parallel with veins (Chapter 2). The present cryo-SEM observation in this chapter confirmed this distribution pattern (Fig. 3-1), and clearly showed that the droplets were retained just on the salt glands (Fig. 3-3).

The shape and size of the droplets were not much different between control and NaCl-treated plants in the present study. However, the previous study showed that ions contained in droplets were different; the counts by EDS of sodium and chlorine were increased greatly with NaCl treatment of the plants (Chapter 2). Under LV-SEM, angular deposits often appeared on the droplet surface (Chapter 2), and they were considered to be salt crystals formed due to the evaporation of water in the droplet. However, such deposits were hardly observed under cryo-SEM; surfaces of the droplets appeared smoother and more spherical under cryo-SEM than under LV-SEM (Figs. 3-1 and 3-3). These findings suggest that the droplets under cryo-SEM were preserved better than under LV-SEM. It is considered that cryo-SEM is an effective method for examining both leaf surfaces and (frozen) liquids on the surfaces (Ensikat *et al*. 2009).

Surfaces of the salt glands having excreted droplets were observed with high resolution by cryo-SEM after washing. As a result, it is clearly shown that the cuticle on cap cells of the salt glands did not have any pores or signs of rupturing (Fig. 3-2a, b). This finding indicates that the salt glands of Rhodes grass excrete salts without structural disintegration of the cuticle. Multicellular salt glands in dicotyledons

accumulate salt-containing water between the gland cells and the covering cuticle, and leak it via the pores (Esau 1977; Thomson *et al*. 1988). The pores occur in the cuticle on the top of the glands and are detectable by SEM (Fahn 1988). Because the salt glands of Rhodes grass have no pores on their cuticle, salt-containing water is thought to permeate the cuticle. The positional relation between the excreted water and the salt glands is shown in a scheme with ultrastructure of the cells described in chapter 1 (Fig. 3-5). The cuticle on the upside region of the cap cell is separated from the cell wall, and an extracellular cavity is formed (Fig. 3-5 *Ca*) (Chapter 1, 2). It is considered that transported ions accumulate continuously in this cavity and lead to solute-linked water movement, which increases the hydrostatic pressure of the solution in the cavity (Kobayashi 2008; Thomson *et al*. 1988; Chapter 2). The increased pressure would allow the solution to permeate from the cavity through the cuticle to the outside in Rhodes grass.

In higher land plants, the cuticular surfaces are commonly covered with the epicuticular waxes forming two- and three-dimensional structures (Koch *et al*. 2008). However, epicuticular waxes are dissolved out with organic solvents during dehydration and critical-point drying for conventional SEM (Fig. 3-2d) (Pathan *et al*. 2008). Additionally, LV-SEM is unable to detect the wax microstructures due to the low resolution (Pathan *et al*. 2008). In contrast to these methods, cryo-SEM is suitable for observing the microstructures of epicuticular waxes clearly (Ensikat *et al*. 2009). In Rhodes grass, epicuticular waxes covered the surfaces of leaf epidermal cells (Fig. 3-2a, c), whereas the wax microstructures were absent on the cuticle of cap cells (Fig. 3-2a, b). This fact is important to understand how the salt glands transude salt-containing water. Wax is hydrophobic chemical substance and serves as effective barrier against water

movement from the plant body to the atmosphere (Koch *et al*. 2008). The lack of epicuticular waxes on the cap cells may mean that the cuticle on the cap cells is more permeable than that on other epidermal cells and allow easy passage of water. On the other hand, it is reported that wax microstructures exist on the surfaces of the bladder type salt glands in the Chenopodiaceae: in *Atriplex* (Troughton and Card 1973; Uchiyama and Sugimura 1985) and in *Chenopodium* (Pathan *et al*. 2008). Presence or absence of epicuticular waxes on the salt glands may be attributed to their mechanism of salt excretion. The bladder cells store salts and water in their vacuole until collapsing themselves (Esau 1977; Fahn 1988). It makes sense that the bladder cells are covered with hydrophobic waxes to block the water diffusion.

Additionally, three-dimensional epicuticular waxes provide water-repellent surface (Ensikat *et al*. 2009). In Rhodes grass, the excreted droplets contacted epidermis just on the top of the papillae and did not spread onto other surfaces of epidermal cells (Fig. 3-3b, d). This finding indicates that the epidermis covered with epicuticular waxes repels the excreted water. In contrast, the cap cell of the salt gland was ensphered in the droplet (Figs. 3-3 and 3-5). The wax-free cuticle of the cap cells may behave as a hydrophilic surface and attract the water on them. These physical relations may explain why the droplets are retained just on the salt glands over a long term without rolling or falling. Although the water may evaporate from excreted droplets continuously, the droplets stayed attached on the salt glands in Rhodes grass. In the Chenopodiaceae, once a bladder cell excretes salts with collapsing (Esau 1977; Fahn 1988), it becomes unable to excrete subsequently because the cell abscises from epidermis. In contrast, because the salt gland of Rhodes grass excretes salts without structural disintegration, it can excrete continuously. We confirmed that droplets were re-excreted on the leaves

after washing supporting the continuous excretion by salt glands of Rhodes grass (Figs. 3-1 and 3-4).

In conclusion, the present cryo-SEM observation revealed that the salt glands of Rhodes grass excrete salts without rupturing or porous structures on the cuticle of the cap cell, and that the cuticle lacks epicuticular waxes. Additionally, the continuous excretion from the salt glands was confirmed with the digital microscope. These observations suggest that the bicellular salt glands of Rhodes grass excrete salt-containing water continuously through the wax-free cuticle. This excretion mechanism is different from that of bladder cells or multicellular glands in dicotyledons.

Figures

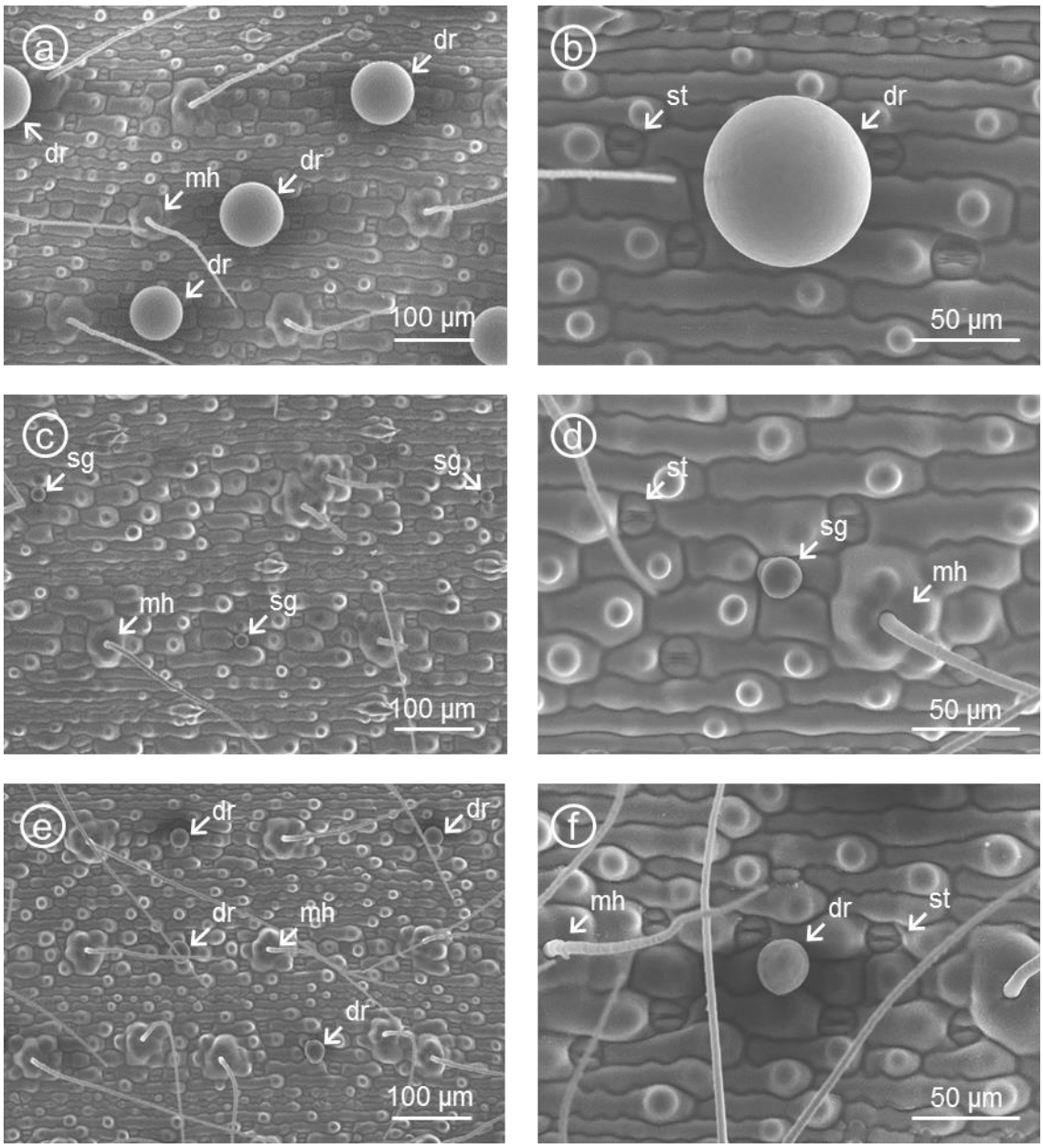

Fig. 3-1.

Abaxial leaf surfaces of Rhodes grass without NaCl treatment (controls) observed by cryo-SEM at 15 kV. (*a*, *b*) Before washing. (*c*, *d*) Just after washing. (*e*, *f*) 24 h after washing. Each observation at different times was conducted on different leaves. Abbreviations: *dr*, droplet; *mh*, macrohair; *sg*, salt gland; *st*, stoma.

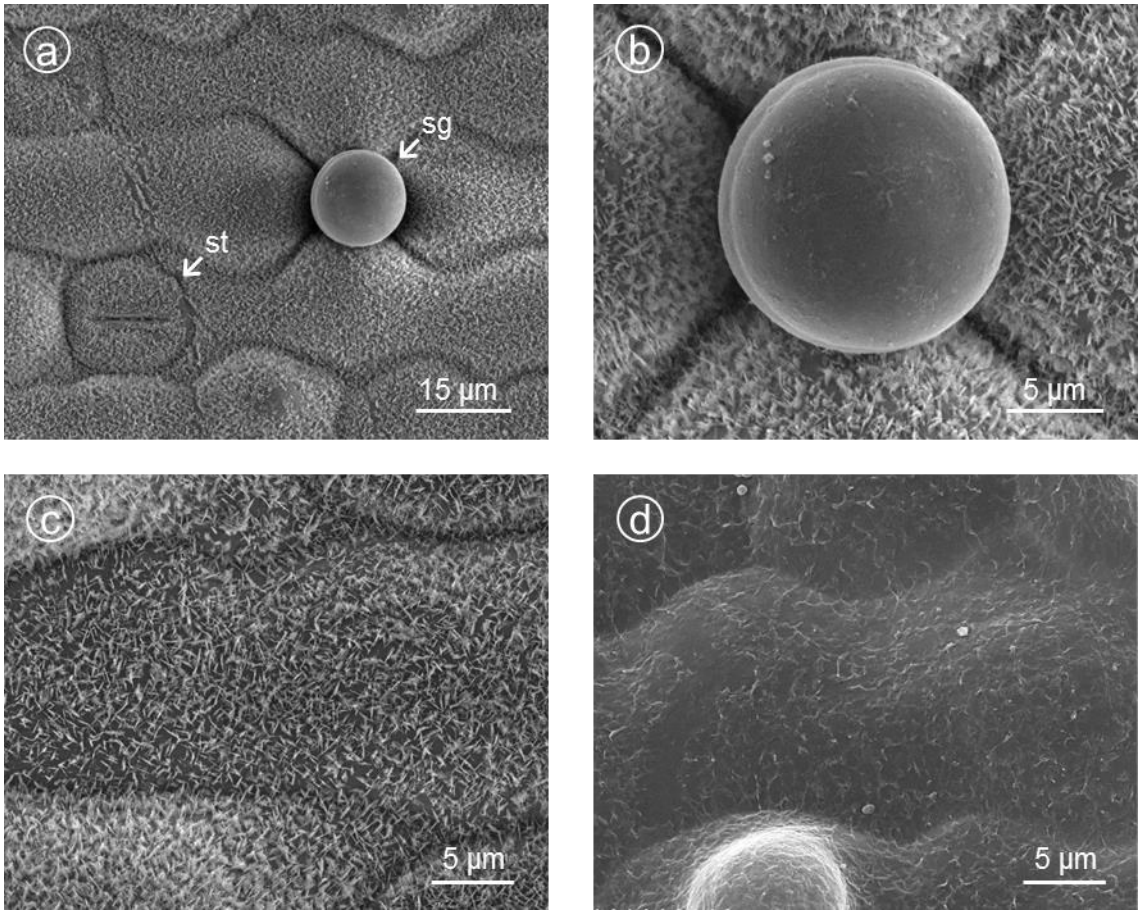

Fig. 3-2.

Washed abaxial leaf surfaces of Rhodes grass treated with 100 mM NaCl. (*a*-*c*) Observed by cryo-SEM at 3 kV. (*a*) Epidermis with a stoma and a salt gland. (*b*) A cap cell of a salt gland with a smooth surface. (*c*) Epidermal cells with wax deposits. (*d*) Epidermal cells without wax deposits observed by conventional SEM; the specimen was chemical fixed, dehydrated, critical-point dried, and coated with gold. Abbreviations: *sg*, salt gland; *st*, stoma.

Note: the stomatal complex of Rhodes grass is composed of two dumbbell-shaped guard cells and two adjacent subsidiary cells. These cells were also covered with wax deposits.

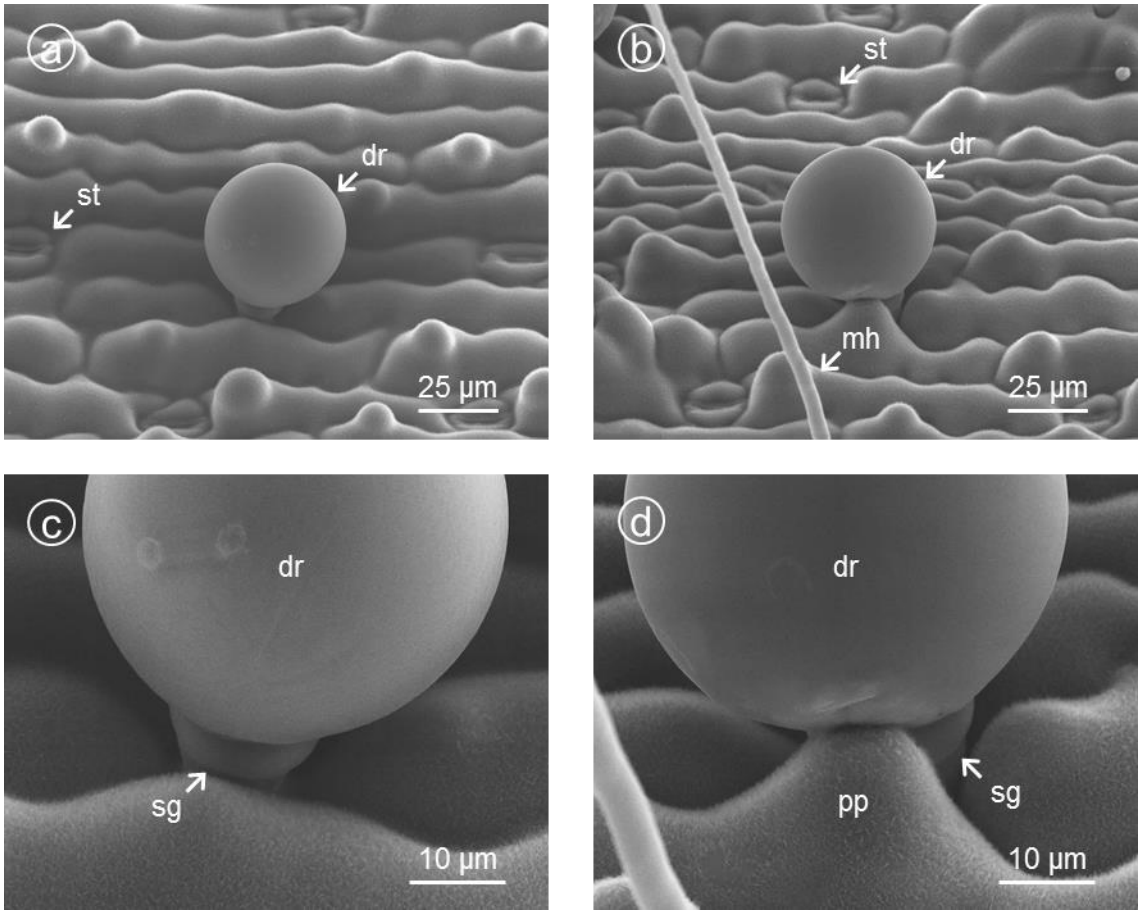

Fig. 3-3.

Inclined views of the unwashed leaf surface and droplets on the surface. Abaxial leaf surfaces of Rhodes grass without NaCl treatment were observed by cryo-SEM at 15 kV, at tilt angle of 45º to the surfaces. (*a*) A droplet on the leaf surface. (*b*) Another droplet on the leaf surface. (*c*, *d*) Enlarged views of pictures *a* and *b*, respectively. (*a*, *c*) The droplet is retained on the cap cell of the salt gland. (*b*, *d*) The droplet is retained on the cap cell and also contacts the top of a papilla. The salt glands are mostly hidden under the droplet. Abbreviations: *dr*, droplet; *mh*, macrohair; *pp*, papilla; *sg*, salt gland; *st*, stoma.

Note: the observation for these figures was conducted on the seventh leaves of Rhodes grass grown for one week shorter than the plants for other observations.

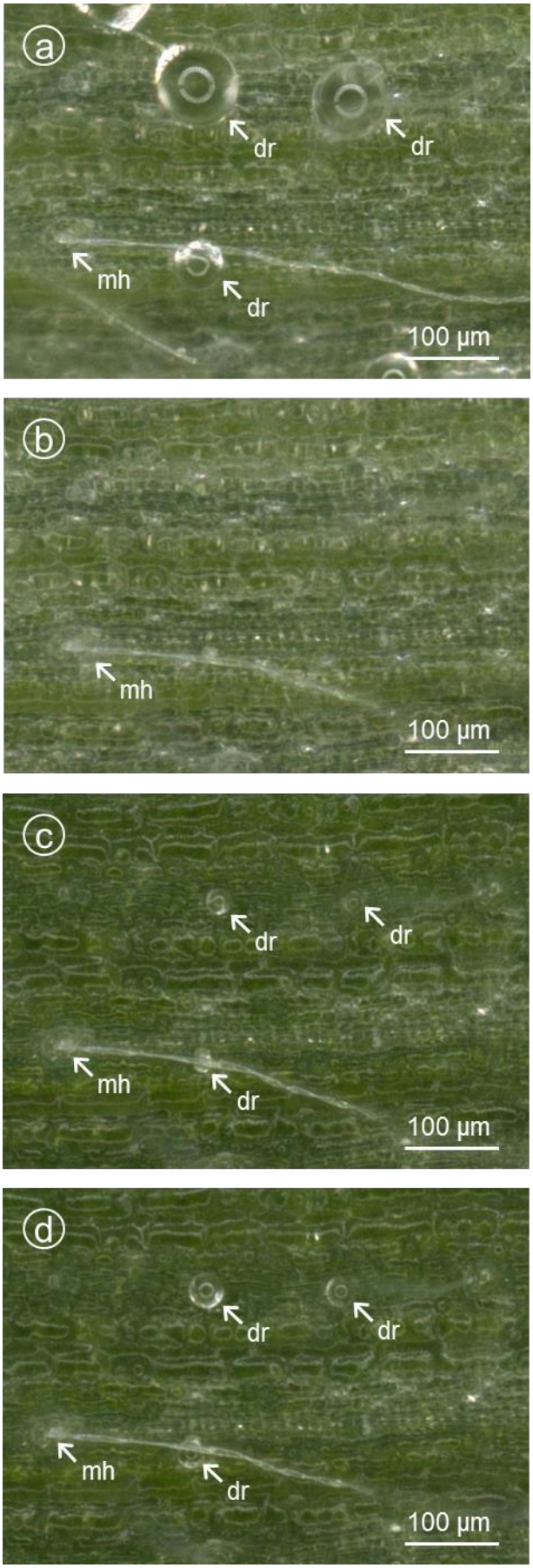

Fig. 3-4.

Excretion on the identical adaxial leaf surface before and after washing the leaf observed with a digital microscope.

(*a*) Before washing with water.

(*b*) Several minutes after washing.

(*c*) 3 h after washing.

(*d*) 6 h after washing.

Abbreviations:

dr, droplet; *mh*, macrohair.

Note:

the ring in the centre of each droplet is the reflection of the illuminator encircling the lens of the digital microscope.

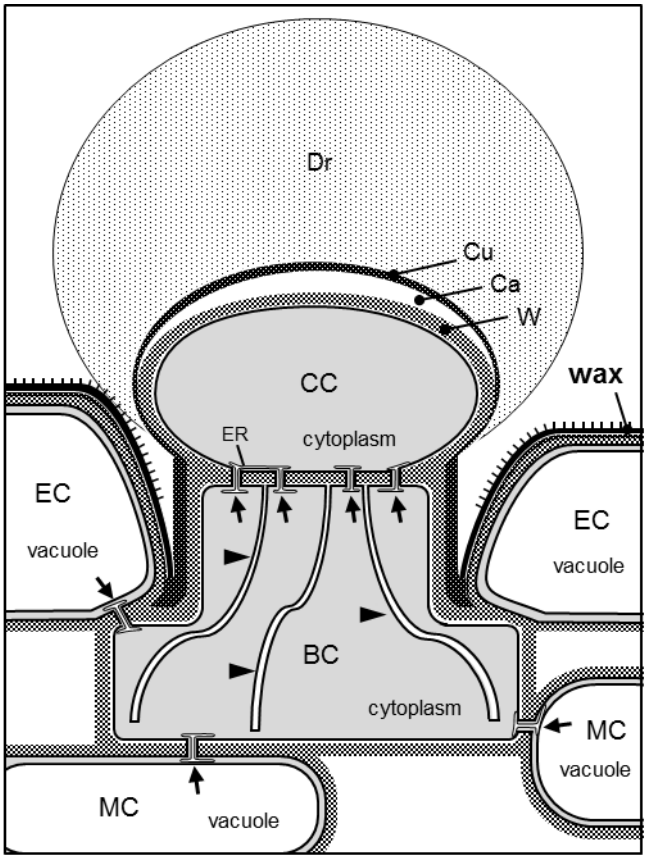

Fig. 3-5.

A schematic explanation of a bicellular salt gland. Abbreviations: *BC*, basal cell; *Ca*, cavity; *CC*, cap cell; *Cu*, cuticle; *EC*, epidermal cell; *ER*, endoplasmic reticulum; *Dr*, droplet; *MC*, mesophyll cell; *W*, cell wall. Arrows indicate plasmodesmata, arrowheads indicate partitioning membranes, and *wax* means epicuticular waxes.

**Modified from Fig. 1-12 in chapter 1.*

General Discussion

In this thesis, I investigated the morphology of the bicellular salt glands of Rhodes grass at the electron-microscopic level and gained new insight into their salt-excretion mechanism, especially the excretion process through the cuticle of cap cells. In chapter 1, I showed the detail features of the salt glands regarding their shape and distribution on the leaves by conventional SEM and regarding their intracellular ultrastructure by TEM. In chapter 2, I demonstrated that the bicellular glands of Rhodes grass really excrete salts as water droplets, on the basis of the observations on fresh leaf surfaces by LV-SEM. In chapter 3, I revealed that the cuticle of the cap cells lacks the epicuticular waxes on their surface and that the cuticle does not have any ruptures or pores, on the basis of the observations by cryo-SEM. Consequently, I proposed that the bicellular glands of Rhodes grass excrete salt-containing water through the permeable cuticle of the cap cell without disintegration of the cuticular structure. Because the glands excrete salts without structural disintegration, the excretion continues after once salts are excreted. The continuous excretion would be caused by active transport in the gland cells, which possess high cytoplasmic density and abundant mitochondria.

The excretion pathway by the active bicellular glands discussed in this thesis is summarized below. (1) The ions are collected from adjacent epidermal and mesophyll cells or their apoplast to the basal cell. (2) The collected ions are then transported to the cap cell via the partitioning membranes, which extend throughout the cytosol in the basal cell as layered sheet-like structures. (3) The ions transported to the cap cell are accumulated in an extracellular cavity, which is formed between the cell wall and the cuticle at the top of the cap cell. (4) The accumulated ions lead to solute-linked water movement, which increases the hydrostatic pressure of the solution in the cavity. (5) As

a result, the salt-containing water permeates from the cavity through the cuticle to the outside due to the pressure.

The partitioning membranes in the basal cells are one of the characteristic structures of the salt gland cells and are believed to have specific roles in salt transport (Chapter 1). Their structure is multi-layered sheets, and their inside space is considered to be continuous with the apoplast between the cap and basal cells (Figs. 1-9b, 1-11, 1-12). Therefore, the partitioning membranes probably amplify the interface between the apoplast and symplast and thereby contribute to increase transport efficiency. In general, bicellular glands in the Chloridoideae have preference of cations for excretion in the following order: Na >> K > Ca > Mg (Kobayashi 2008). The selective transport supports the notion that the ions are excreted across membranes in the gland cells. In addition to the selective transport, active transport is expected to function. The abundant mitochondria observed in the basal cell would supply energy for ion-transport across the apoplast/symplast interface (Chapter 1). In addition, it was reported that the salt-excretion ability is decreased in the leaves treated with inhibitors of ion transporters or of ATP synthase (Kobayashi *et al*. 2007; Kobayashi and Masaoka 2008). For the above reasons, the partitioning membranes are predicted to have active ion transport proteins, such as H^+-ATPase, Na^+-H^+ antiporter, or high-affinity K^+ transporter. These membrane proteins transport ions against the concentration gradient (Taiz and Zeiger 2002). It was reported that bladder cells in the Chenopodiaceae have higher activities of the tonoplast H^+-ATPase (V-ATPase) and of the Na^+-H^+ antiporter compared to other leaf cells (Barkla *et al*. 2002). High H^+-ATPase activity is also reported in *S. virginicus* (Poaceae) (Naidoo and Naidoo 1999). However, localization of these transport proteins in the salt glands of the Poaceae has not been elucidated yet. Further investigation

focused on the transport proteins is needed to understand the role of the basal cell in salt-excretion pathway.

Although it is shown that the cap cell of the bicellular gland really excretes salts (Chapters 2 and 3), the excretion pathway from the basal cell to the extracellular cavity at the top of the cap cell has not been characterized. There are several conflicting hypotheses in this process (Levering and Thomson 1971; Oross *et al.* 1985; Naidoo and Naidoo 1998b, 1999; Kobayashi 2008; Semenova *et al*. 2010; *see discussion in chapter 1*). Because the cap cell has no specific membrane structures increasing its surface area such as the partitioning membranes in the basal cell (Figs. 1-9 and 1-10), the cytosol of the cap cell may not actually contribute to the ion-transport actively; the cap cell may have roles to support the physiological metabolism of the basal cell.

There is a possibility that the cap cell contributes not only to the salt-excretion but also to other unknown metabolisms, as a part of the microhair. Microhairs are bicellular trichomes existing in most of the Poaceae except for the subfamily Pooideae (Tateoka *et al*. 1959; Clayton and Renvoize 1986) and function as salt glands in some salt-tolerant Poaceae plants mainly belonging to the Chloridoideae (Kobayashi 2008). Although staple crops, such as rice, maize, sorghum, and millet, also possess microhairs (Clayton and Renvoize 1986), the biological significance of the microhairs in these salt-sensitive crops has not been known well. Some histochemical studies confirmed that the microhair possessing a low ability to excrete ions could secrete metabolites, such as polysaccharides and proteins (Amarasinghe 1990; McWhorter *et al*. 1995). However, it is pointless to discuss in detail on the functions of these metabolite secretions because of few conclusive chemical analyses (Amarasinghe 1990). To better understand the biological significance of the microhairs in the Poaceae, it is also needed to investigate

metabolite-secretion in more detail. Furthermore, interspecific comparison of ultrastructure between salt-excreting and metabolite-secreting microhairs in the Poaceae would provide beneficial cues for applying salt-excreting ability to the microhair of salt-sensitive Poaceae crops to improve salt tolerance.

The excretion mechanism via a salt gland is covered in this thesis, whereas the differentiation mechanism of the gland cells during the formation of leaf tissues has not been discussed in detail. It is also important to know how a plant regulates number of their glands, because the total amount of salt excretion is determined by a product of two factors: the efficiency of excretion per gland and total number of glands (Ding *et al.* 2009). In addition, understanding the regulation mechanism of gland number is necessary for applying the salt-excretion function to practical improvement in salt tolerance of crops, because the salt-excretion process would consume energy and also lose water excreted together with salts (Chapters 1 and 3). Compared with bladder cells that are densely-distributed on the leaf surfaces and covered them entirely (Troughton and Card 1973; Uchiyama and Sugimura 1985), bicellular glands are sparsely-distributed on the leaf surfaces (Figs. 1-4, 2-1, 2-2, and 3-1; Oross and Thomson 1982; Marcum and Murdoch 1989; Barhoumi *et al*. 2007; Kobayashi *et al.* 2010). This difference in distribution density is attributed to a variation in excretion mechanism; bladder cells excrete salts with collapsing (Esau 1977; Fahn 1988) and abscise from epidermis, whereas bicellular glands excrete salts without structural disintegration and continue to excrete (Chapter 3). This continuous excretion mechanism would need fewer glands and lead to resource saving. Interestingly, the number of salt glands was increased with NaCl treatment on adaxial leaf surface (Figs. 1-5). In contrast, it is reported that the number of the glands was decreased with jasmonates, which is a

signaling factor of herbivore attacks (Kobayashi *et al*. 2010). Although the number of salt glands is changed in response to external factors, their physiological mechanisms are obscure. It is particularly interesting to determine whether signaling factors for salinity stress such as reactive oxygen species or abscisic acid could affect the number of the salt glands.

Finally, I would emphasize the potential of the Rhodes grass as a model plant to investigate bicellular salt glands in the Poaceae. Because Rhodes grass is cultivated as fodder worldwide, knowledge of the grass has been accumulated for various purposes based on agricultural demands. Recently, Rhodes grass is considered an attractive model species for genome analysis among the forage grass because of its relatively small genome size (Ubi *et al.* 2001; Tsuruta and Ebina 2009). Although there are currently few studies based on the molecular biological analysis of salt excretion via bicellular glands in the Poaceae (Kobayashi 2008), genetic analysis with Rhodes grass will make a breakthrough in this research. To understand salt-excretion mechanisms, further studies are needed to link morphological features of bicellular glands with physiological or genetical phenomena. I hope that this study becomes the basis for the investigations into the salt-excretion mechanisms by the bicellular gland in the Poaceae and contributes to improving the salt tolerance of crops.

References

Amarasinghe V., Watson L., 1988. Comparative ultrastructure of microhairs in grasses. *Botanical Journal of the Linnean Society* 98: 303–319.

Amarasinghe V., Watson L., 1989. Variation in salt secretory activity of microhairs in grasses. *Australian Journal of Plant Physiology* 16: 219–229.

Amarasinghe V., 1990. Polysaccharide and protein secretion by grass microhairs. *Protoplasma* 156: 45–56.

Barhoumi Z., Djebali W., Smaoui A., Chaïbi W., Abdelly C., 2007. Contribution of NaCl excretion to salt resistance of *Aeluropus littoralis* (Willd) Parl. *Journal of Plant Physiology* 164: 842–850.

Barhoumi Z., Djebali W., Abdelly C., Chaïbi W., Smaoui A., 2008. Ultrastructure of *Aeluropus littoralis* leaf salt glands under NaCl stress. *Protoplasma* 233: 195–202.

Barkla B.J., Vera-Estrella R., Camacho-Emiterio J., Pantoja O., 2002. Na^+/H^+ exchange in the halophyte *Mesembryanthemum crystallinum* is associated with cellular sites of Na^+ storage. *Functional Plant Biology* 29: 1017–1024.

Chaves M.M., Flexas J., Pinheiro C., 2009. Photosynthesis under drought and salt stress: regulation mechanisms from whole plant to cell. *Annals of Botany* 103: 551–560.

Clayton W.D., Renvoize S.A., 1986. *Genera Graminum: Grasses of the World.* Her Majesty's Stationery Office, London.

Dietrich D., Hinke S., Baumann W., Fehlhaber R., Bäucker E., Rühle G., Wienhaus O., Marx G., 2003. Silica accumulation in *Triticum aestivum* L. and *Dactylis glomerata* L.. *Analytical and Bioanalytical Chemistry* 376: 399–404.

Ding F., Song J., Ruan Y., Wang B., 2009. Comparison of the effects of NaCl and KCl at the roots on seedling growth, cell death and the size, frequency and secretion

rate of salt glands in leaves of *Limonium sinense*. Acta Physiologiae Plantarum 31: 343–350.

Ensikat H.J., Schulte A.J., Koch K., Barthlott W., 2009. Droplets on superhydrophobic surfaces: visualization of the contact area by cryo-scanning electron microscopy. *Langmuir* 25: 13077–13083.

Esau K., 1977. *Anatomy of Seed Plants*, 2nd edition. John Wiley and Sons, New York.

Fahn A., 1988. Secretory tissues in vascular plants. *New Phytologist* 108: 229–257.

Hillel D., 2000. *Salinity Management for Sustainable Irrigation: Integrating Science, Environment, and Economics.* World Bank, Washington DC.

Jørgensen H.J.L., Lyshede O.B., Allerup S., 1995. Epicuticular wax of the first leaves of two barley cultivars studied by cryo scanning electron microscopy. *Journal of Agronomy and Crop Science* 174: 217–224.

Kobayashi H., Masaoka Y., Takahashi Y., Ide Y., Sato S., 2007. Ability of salt glands in Rhodes grass (*Chloris gayana* Kunth) to secrete Na^+ and K^+. *Soil Science and Plant Nutrition* 53: 764–771.

Kobayashi H., 2008. Ion secretion via salt glands in Poaceae. *Japanese Journal of Plant Science* 2: 1–8.

Kobayashi H., Masaoka Y., 2008. Salt secretion in Rhodes grass (*Chloris gayana* Kunth) under conditions of excess magnesium. *Soil Science and Plant Nutrition* 54: 393–399.

Kobayashi H., Yanaka M., Ikeda T.M., 2010. Exogenous methyl jasmonate alters trichome density on leaf surfaces of Rhodes grass (*Chloris gayana* Kunth). *Journal of Plant Growth Regulation* 29: 506–511.

Koch K., Bhushan B., Barthlott W., 2008. Diversity of structure, morphology and wetting of plant surfaces. *Soft Matter* 4: 1943–1963.

Levering C.A., Thomson W.W., 1971. The ultrastructure of the salt gland of *Spartina foliosa*. *Planta* 97: 183–196.

Liphschitz N., Waisel Y., 1974. Existence of salt glands in various genera of the Gramineae. *New Phytologist* 73: 507–513.

Liphschitz N., Shomer-Ilan A., Eshel A., Waisel Y., 1974. Salt glands on leaves of Rhodes grass (*Chloris gayana* Kth.). *Annals of Botany* 38: 459–462.

Lüttge U., 1971. Structure and function of plant glands. *Annual Review of Plant Physiology* 22: 23–44.

Marcum K.B., Murdoch C.L., 1990. Salt glands in the Zoysieae. *Annals of Botany* 66: 1–7.

McWhorter C.G., Ouzts C., Paul R.N., 1993. Micromorphology of Johnsongrass (*Sorghum halepense*) leaves. *Weed Science* 41: 583–589.

McWhorter C.G., Paul R.N., Ouzts J.C., 1995. Bicellular trichomes of Johnsongrass (*Sorghum halepense*) leaves: morphology, histochemistry, and function. *Weed Science* 43: 201–208.

Naidoo G., Naidoo Y., 1998a. Salt tolerance in *Sporobolus virginicus*: the importance of ion relations and salt secretion. *Flora* 193: 337–344.

Naidoo Y., Naidoo G., 1998b. *Sporobolus virginicus* leaf salt glands: morphology and ultrastructure. *South African Journal of Botany* 64: 198–204.

Naidoo Y., Naidoo G., 1999. Cytochemical localisation of adenosine triphosphatase activity in salt glands of *Sporobolus virginicus* (L.) Kunth. *South African Journal of Botany* 65: 370–373.

Neumann P.M., 2011. Recent advances in understanding the regulation of whole-plant growth inhibition by salinity, drought and colloid stress. *Advances in Botanical Research* 57: 33–48.

Oross J.W., Thomson W.W., 1982a. The ultrastructure of Cynodon salt glands: the apoplast. *European Journal of Cell Biology* 28: 257–263.

Oross J.W., Thomson W.W., 1982b. The ultrastructure of the salt glands of *Cynodon* and *Distichlis* (Poaceae). *American Journal of Botany* 69: 939–949.

Oross J.W., Leonard R.T., Thomson W.W., 1985. Flux rate and a secretion model for salt glands of grasses. *Israel Journal of Botany* 34: 69–77.

Parida A.K., Das A.B., 2005. Salt tolerance and salinity effects on plants: a review. *Ecotoxicology and Environmental Safety* 60: 324–349.

Pathan A.K., Bond J., Gaskin R.E., 2008. Sample preparation for scanning electron microscopy of plant surfaces – horses for courses. *Micron* 39: 1049–1061.

Read N.D., Jeffree C.E., 1991. Low-temperature scanning electron microscopy in biology. *Journal of Microscopy* 161: 59–72.

Rengasamy P., 2010. Soil processes affecting crop production in salt-affected soils. *Functional Plant Biology* 37: 613–620.

Semenova G.A., Fomina I.R., Biel K.Y., 2010. Structural features of the salt glands of the leaf of *Distichlis spicata* ‘Yensen 4a’ (Poaceae). *Protoplasma* 240: 75–82.

Somaru R., Naidoo Y., Naidoo G., 2002. Morphology and ultrastructure of the leaf salt glands of *Odyssea paucinervis* (Stapf) (Poaceae). *Flora* 197: 67–75.

Soni S.L., Kaufman P.B., Jones R.A., 1972. Electron microprobe analysis of the distribution of silicon and other elements in rice leaf epidermis. *Botanical Gazette* 133: 66–72.

Spurr A.R., 1969. A low-viscosity epoxy resin embedding medium for electron microscopy. *Journal of Ultrastructure Research* 26: 31–43.

Suttie J.M., 2000. *Hay and Straw Conservation: For Small-scale Farming and Pastoral Conditions*, FAO Plant Production and Protection Series 29. Food and Agriculture Organization of the United Nations, Rome.

Taiz L., Zeiger E., 2002. *Plant Physiology*, 3rd edition. Sinauer Associates, Sunderland.

Tanaka K., Naguro T., 1981. High resolution scanning electron microscopy of cell organelles by a new specimen preparation method. *Biomedical Research* 2 (Suppl.): 63–70.

Tateoka T., Inoue S., Kawano S., 1959. Notes on some grasses. IX. systematic significance of bicellular microhairs of leaf epidermis. *Botanical Gazette* 121: 80–91.

Thomson W.W., Faraday C.D., Oross J.W., 1988. Salt glands. In: Baker, D.A., Hall, J.L. (Eds.), *Solute Transport in Plant Cells and Tissues*. Longman Scientific and Technical, Essex, 498–537.

Troughton J.H., Card K.A., 1974. Leaf anatomy of *Atriplex buchananii*. *New Zealand Journal of Botany* 12: 167–177.

Tsuruta S., Ebina M., 2009. Breeding and forage utilization of Rhodes grass (*Chloris gayana* Kunth). *Japanese Journal of Grassland Science* 55: 188–195 (*in Japanese*).

Ubi B.E., Fujimori M., Ebina M., Komatsu T., 2001. Amplified fragment length polymorphism analysis in diploid cultivars of rhodesgrass. *Plant Breeding* 87: 85–87.

Uchiyama Y., Sugimura Y., 1985. Salt-excreting function of vesiculated hairs of *Atriplex nummularia*. *Japanese Journal of Crop Science* 54: 39–46 (*in Japanese with English summary*).

Waisel Y., 1972. *Biology of Halophytes*. Academic Press, New York and London.

Werker E., 2000. Trichome diversity and development. *Advances in Botanical Research* 31: 1–35.

Acknowledgements

I would like to express my sincere appreciation to Dr. Mitsutaka Taniguchi, Professor of Nagoya University, for providing me to valuable advice and for encouraging me to study freely and vigorously.

I also wish to express my deepest sense of gratitude to Dr. Hiroshi Miyake, Emeritus Professor of Nagoya University, for equipping me with essential technique of plant-anatomy and for providing me to valuable suggestions. I would never accomplish this study without him.

I am grateful to Dr. Katsuya Yano of Crop Science Laboratory, Nagoya University for the use of an atomic absorption spectrometer and a digital microscope, and for having lively discussions about my study. I express my special thanks to Dr. Kanjun Hirunagi and Masumi Nozaki of The Nagoya University Museum for the use of SEM (TM-1000) and EDS.

I thank to Dr. Shingo Hata, Dr. Michio Kawasaki, Dr. Shiro Mitsuya, Dr. Koji Yamane, Dr. Koichi Tsutsumi, Dr. Jannatul Ferdose, and Dr. Eiji Omoto for valuable discussions in connection with this study. Special thanks are expressed Yoshiko Yamaguchi for her cheerful encouragement and valuable advice for my first paper.

I would also like to express my gratitude to Daiko Foundation for granting me a financial support in 2012 and to Nagoya University Academic Encouraging Prize for providing me a financial support in 2013.

Lastly, I express my heartfelt thanks to my colleagues in Graduate School of Bioagricultural Sciences for their kindness and encouragement to support me.

February, 2014　Takao Oi